Overexpression of neuronal K^+-Cl^- co-transporter enhances dendritic spine plasticity and motor learning

中村　佳代

博士（医学）

総合研究大学院大学
生命科学研究科
生理科学専攻

平成３０（２０１８）年度

論文題目

Overexpression of neuronal K^+-Cl^- co-transporter enhances dendritic spine plasticity and motor learning

Nakamura, Kayo

SOKENDAI (The Graduate University for Advanced Studies)

Department of Physiological Sciences

School of Life Science

2018

Contents

Abstract

The neuron-selective isoform of the K^+-Cl^- cotransporter KCC2 plays an important role in regulating intracellular chloride concentration. In most adult neurons KCC2 simultaneously exports K^+ and Cl^- and thereby maintains a low intracellular Cl^- that facilitates subsequent gamma-amino butyric acid receptor ($GABA_A$Rs) mediated Cl^- influx, hyperpolarization and neuronal inhibition. Indeed, GABAergic inhibition can be diminished when KCC2 is absent or has reduced function, such as occurs during neuronal development and/or after injury. Given this role in influencing GABA function, there has been extensive investigation into the contributions that KCC2 may play in neuronal circuit development and in the pathogenesis of different diseases, and into the mechanisms which regulate KCC2 expression and transport function.

However, KCC2 has also been reported to have additional morphogenic effects on neuronal circuits independent of its Cl^- transport function. In neuronal cultures from KCC2 knockout mice, dendritic spines exhibited a more immature filopodia-like phenotype, and the number of immunohistochemically and functionally identified excitatory synapses was markedly decreased. Remarkably, this immature spine phenotype was rescued by overexpression of transport-deficient KCC2 mutant constructs. Furthermore, *in utero* overexpression of KCC2, or a transport-defective mutant KCC2, resulted in an increase in the density of mature dendritic spines in the somatosensory

cortex (Layer II/III) that was sustained for at least until 90 days after birth. Pertinently, KCC2 appears to form a complex with the actin-associated proteins 4.1N and βPIX, and can interact with the kinase and cofilin signaling pathways associated with spine development and stabilization. Thus it would appear that KCC2 supports the development of excitatory synapses by enhancing spinogenesis and/or maturation. Such a role is consistent with the upregulation of KCC2 expression in development coinciding with the start of spinogenesis, and may (at least partly) explain the presence of KCC2 on dendritic spines at glutamatergic synapses.

Maintenance of dendritic spines in the adult nervous system is also highly dynamic, underpinned by numerous molecular mechanisms, and facilitates the functional and structural plasticity required for memory and behavioral adaptations in response to training. More specifically, *in vivo* experiments have demonstrated a strong correlation between the rate of newly-formed dendritic spines in the motor cortex and the extent and rate at which mice can improve specific motor behaviors during learning. In addition, long-term potentiation (LTP) of synaptic transmission is associated with the appearance of new dendritic spines and an increase in the volume of dendritic spine heads, while long-term depression (LTD) is correlated with dendritic spine shrinkage and removal. Together this suggests an activity-dependent modulation of dendritic spine appearance, growth and stability during learning. Recent evidence suggests that KCC2 can directly contribute to aspects of dendritic spine plasticity. Suppression of KCC2 expression in juvenile rats and in cultured

neurons prevented the induction of LTP and the associated increases in dendritic spine volume and AMPA receptor insertion, pointing to a possible link between KCC2 and learning induced synaptic plasticity in adult neuronal circuits.

Here, I examined the effects of KCC2 expression on synaptic plasticity in the motor cortex (M1) and motor learning *in vivo*. I used a genetically modified mouse that overexpression of KCC2 under the control of Ca^{2+}/calmodulin-dependent protein kinase II (CaMK2) promoter by combining KCC2-tetO knock-in mouse and CaMK2-tTA mouse (CaMK2-tTA/tetO-KCC2 mice$^{+/+}$: KCC2 overexpressing mice). Firstly, in order to confirm the overexpression of KCC2 in these mice, I examined the expression of KCC2 protein using western blotting and immunohistochemistry. At 7 days after stopping the oral administration of the tetracycline derivative, doxycycline (Dox), relative value of total KCC2 was significantly increased in the cerebral cortex. As the functional relevance, during repetitive stimulation applied to inhibitory afferents to cortical pyramidal neurons, the attenuation of evoked inhibitory postsynaptic currents IPSC in amplitude was significantly less in KCC2 overexpressing neurons than in WT neurons, suggesting more potent maintenance of low intracellular Cl^- in KCC2 overexpressing mice. Next, I evaluated the anxiety and the behavioral activity with open field test and elevated plus maze test. There was no significant difference both in the anxiety and the activity behavior between KCC2 overexpressing and WT mice. On the other hand, the rotarod training test, which is employed to assess motor coordination and learning, KCC2

overexpressing mice showed a significantly greater motor learning compared to WT mice. *In vivo* imaging with two-photon laser microscopy revealed that the formation rate of dendritic spines of layer V pyramidal neurons gradually increased in KCC2 overexpressing and WT mice with training. Spine formation rate of KCC2 overexpressing mice, but not the WT mice, after the first training significantly increased compared with that before training. Corresponding with the increased spine formation in KCC2 overexpressing mice, the spine turnover rate (an average of elimination and formation) after 1 day of training was also significantly increased in KCC2 overexpressing mice, but not in WT mice. Hence my data supports the growing appreciation of the transport-independent role of KCC2 in dendritic spine development/maturation/ maintenance, suggesting a putative role in enhancing synaptic plasticity and performance during learning *in vivo*.

Introduction

Neuronal K^+-Cl^- cotransporter KCC2 has an important role in regulating intracellular Cl^- concentration of the neurons. It is the molecule which simultaneously excludes K^+ and Cl^- toward extracellular space (Delpire, 2000; Kaila, 1994). This protein has been known to express in mature neurons but less in immature neurons, and thus regulates the developmental switch of gamma-aminobutyric acid (GABA) response from depolarization to hyperpolarization (Kakazu et al., 1999; Rivera et al., 1999; Ueno et al., 2002). Gradually rise of KCC2 expression at the hippocampus around postnatal two weeks in rodents (Ludwig et al., 2003) is temporally fitting with the synaptogenesis in the development at these areas of brain. Previous paper suggested that the distribution of KCC2 has highly localized near GABAergic synapses, and more in dendritic spine near glutamatergic synapse (Chamma et al., 2013; Gulyas et al., 2001).

Recently, KCC2 has been found to be a molecule involved in synaptogenesis besides its Cl^- transported function. Declining expression of KCC2 after 2 weeks in culture cells induces more filopodia showing immature-like protrusions, compared with WT neuron, and decreased the number of functional excitatory synapses (Lee et al., 2007). Instead, overexpression of KCC2 in mice Layer II/III pyramidal neurons from perinatal period results in increased number of functional excitatory synapses in mature period (Fiumelli et al., 2013). Morphogenesis role of KCC2 is mediated by its

C-terminal. C-terminus of KCC2 directly interacts with the actin -associated protein 4.1N, and regulates structural maturation of dendritic spines via interacting with actin, spectrin, and alpha -amino-3-hydroxy-5-methyl-4-isoxazolepropionic acid (AMPA) -type glutamate receptor (Lee et al., 2007; Penzes, 2007). In fact, chronic KCC2 suppression after spine morphogenesis in mature neurons relieved a constraint to the lateral diffusion and aggregation of postsynaptic AMPA -type glutamate receptor (Gauvain et al., 2011). Pertinently, KCC2 also appears to form a complex with the βPIX, and can interact with the kinase and cofilin signaling pathways associated with spine development and stabilization. Thus, it would appear that KCC2 supports the development of excitatory synapses by enhancing spinogenesis and/or maturation. Such a role is consistent with the upregulation of KCC2 expression in development coinciding with the start of spinogenesis, and may (at least partly) explain the presence of KCC2 on dendritic spines at glutamatergic synapses.

Maintenance of dendritic spines in the adult nervous system is also highly dynamic, underpinned by numerous molecular mechanisms, and facilitates the functional and structural plasticity required for memory and behavioral adaptations in response to training (Holtmaat and Svoboda, 2009; Kasai et al., 2010; Yu and Zuo, 2011). More specifically, *in vivo* experiments have demonstrated a strong correlation between the rate of newly-formed dendritic spines in the motor cortex and the extent and rate at which mice can improve specific motor behaviors during learning (Xu et al., 2009; Yang et al., 2009). In addition, long-term potentiation (LTP) of synaptic

transmission is associated with the appearance of new dendritic spines and an increase in the volume of dendritic spine heads, while long-term depression (LTD) is correlated with dendritic spine shrinkage and removal (reviewed in Kasai et al (Kasai et al., 2010). and Bosch and Hayashi (Bosch and Hayashi, 2012)). Together, this suggests an activity-dependent modulation of dendritic spine appearance, growth and stability during learning. Recent evidence suggests that KCC2 can directly contribute to aspects of dendritic spine plasticity. Suppression of KCC2 expression in juvenile rats and in cultured neurons prevented the induction of LTP and the associated increases in dendritic spine volume and AMPA receptor insertion (Chevy et al., 2015), pointing to a possible link between KCC2 and learning induced synaptic plasticity in adult neuronal circuits.

Therefore, to address whether altered KCC2 modulates dendritic spine and synaptic plasticity in adult animals, I have utilized a transgenic mouse wherein KCC2 can be conditionally overexpressed by altering dietary doxycycline. I overexpressed KCC2 and quantified the effects of this on dendritic spine density. Furthermore, I examined how overexpressed KCC2 affects dendritic spine plasticity during motor learning and its functional implications. I hypothesized that increasing KCC2 levels in the adult brain would increase the density of dendritic spines, as seen in developing brains. I also proposed that increasing KCC2 would enhance the dendritic spine plasticity associated with motor learning. Using *in vivo* two photon imaging of dendrites and spines in apical dendrites of layer V motor cortex pyramidal neurons, I show that overexpression of KCC2 does indeed increase

spine density. Using time-lapse imaging I then demonstrate that KCC2 overexpression increases dendritic spine formation in the motor cortex during rotarod motor learning and increases the extent and rate at which rotarod performance is enhanced during training.

Materials and Methods

All animal experiments were carried out according to the guidelines defined by the National Institutes of Natural Sciences (NIPS), and approved by the Okazaki Institutional Animal Care and Use Committee, or by the UNSW Sydney Animal Care and Ethics Committee.

Animals

I used a conditional transgenic mouse in which overexpression of KCC2 which is under CaMK2 promoter can be induced by cessation of dietary supplementation with doxycycline (Goulton et al., 2018). KCC2 expression was driven by the tetracycline transactivator (tTA) binding to the tetracycline operator construct (tet-O), and this interaction is prevented by doxycycline (Gossen and Bujard, 1992). The tet-O construct was introduced upstream of the KCC2 gene, and KCC2 overexpression was restricted to excitatory neurons of the forebrain by using the CaMKIIα promoter to drive tTA expression (Mayford et al., 1996). Mice were housed in standard cages with a reversed light/dark cycle (light on 6:00 A.M., light off 6:00 P.M.) and fed with doxycycline (Dox, 100 mg/kg) laced chow. Adult (8-12 week old) male mice were used for experiments, and feed was exchanged to Dox-free standard chow prior to experiments as indicated (typically 2-3 weeks).

Behavioral Tests: The Open Field Test and The Elevated Plus Maze

Male mice were singly standard housed and they were acclimatized over 30 minute before behavioral tests in testing room. They were subjected to the open field test on day 1, and elevated plus maze test performed on day 2.

The Open Field Test

Measurement of spontaneous activity with open field test reveals locomotion and anxious state of mice. The open field box made of a square white box (40 cm x 40 cm x 40 cm). The center area (24 cm x 24 cm) was consisted of 36% of the field area. A single animal was placed into the box for 10 minutes. Overall activity in the box was measured via a USB camera (Logicool HD 720p, Logitech, Japan). The ratio of total distance traveled were analyzed with Anymaze software (Woods Dale, Illinois).

The Elevated Plus Maze

This test assesses anxiety-like behavior and free searched movement in four of the arms by using the property that mice prefer walls and avoid high places. Two of the arms had 130 cm long laneways of 10 cm width with walls of 10 cm height, whereas the two arm consists without walls. All animals were placed in the center at start and were permitted to search freely for 10 minutes. Overall activity on the arms was recorded and tracked by USB camera (Logicool HD 720p, Logitech, Japan). The distance traveled, and the number of entries of open arm were analyzed with Anymaze

software (Woods Dale, Illinois).

Accelerating Rotarod test

One week prior to behavioral experiments, mice were identified, weighed and health-checked, before being acclimatized to the behavioral rooms for at least 30 mins prior to testing. The accelerating rotarod test used a rotarod with five lanes, as previously described in Kakegawa et al (Kakegawa et al., 2011), and Rothwell et al (Rothwell et al., 2014). Mice were placed into the rotarod and the rotation speed was increased from 4 to 40 rotations per minute (r.p.m) over 5 minutes. The time at which a mouse fell from the rotarod was recorded. Six trials were performed over a period of 90 mins, and this was repeated daily over 5 successive days.

Surgery and virus injection for *in vivo* imaging

To facilitate *in vivo* imaging, I made cranial windows over M1 motor cortex using the open skull approach as described in Kim et al (Kim et al., 2016). and Wake et al (Wake et al., 2009). Surgery was performed over 2 days, 2-3 weeks before imaging and rotarod experiments. On the first surgery day, a metal head-plate, used to secure the mouse head under the microscope objective lens, was mounted with dental cement onto exposed skull under anesthesia (ketamine:xyalizine mix, 0.13: 0.01 mg/g, i.p.). On the second surgery day, the skull over the M1 motor cortex was removed under anaesthesia (isoflurane, 1.5% vol/vol in air), leaving a 2.0-3.0 mm diameter window centered at 1.5

mm lateral to Bregma and corresponding to the mouse's forepaw. Subsequently, adeno-associated virus (AAV) containing an enhanced green fluorescent protein (eGFP) coupled to a CaMKIIα promoter (AAV2-CaMK2-eGFP (University of Pennsylvania vector core) was injected into layer V of the motor cortex (250 nL over 5 mins). After injection, the cortical surface was washed with artificial cerebrospinal fluid for more than 20 minutes before the open window was sealed using double cover glass and 2-5% agarose. The cover glass was then secured to the adjacent skull using dental cement and cyanoacrylate glue.

Two-photon imaging of dendrites and spines *in vivo*

Mice were anaesthetized with isoflurane (~ 1.5% v/vol in air) and secured via their head-plate under the microscope objective lens. The motor cortex was initially imaged at low resolution at a depth of 500-600 μm to identify eGFP-expressing layer V pyramidal neurons. The apical dendrites of these neurons were traced towards the brain surface and higher resolution imaging of dendrites and spines performed within 100 μm from the cortical surface. On average, 2-5 apical dendrites were imaged in each mouse.

Dendritic spine analysis *in vivo*

Dendrites and spines structures were analyzed as described in Kim et al (Kim et al., 2016).

and Kim and Nabekura (Kim and Nabekura, 2011) using ImageJ (http://rsbweb.nih.gov/ij/). Briefly, I manually identified any dendritic protrusion and classified all these protrusions as spines regardless of length or shape. Thin filopodia without clear spine heads were excluded. Spine formation and elimination rates were determined as the percentages of spines in a single dendrite that appeared or disappeared, respectively, between two successive imaging sessions, and was expressed relative to the total spine number in the former session. Spine turnover was defined as the average number of formed and eliminated spines.

Immunostaining method

Mice were deeply anesthetized (ketamine:xyalizine mix, 0.13: 0.01 mg/g, i.p.) and cardiac perfused with phosphate-buffered saline (PBS) followed by 4% paraformaldehyde. Brains were dissected out and stored in 4% paraformaldehyde at 4^{o}C overnight which was replaced with 30% w/vol sucrose the next day. Brains were then frozen with liquid nitrogen and cut at 35 μm thickness using a microtome and stored at 4^{o}C in PBS. Immunostaining was conducted using primary antibodies anti-NeuN (Mouse, Monoclonal, Millipore, 1:500 dilution) and anti-VP16, amino acids 413-490 (Rabbit, Polyclonal, Abcam, 1:100 dilution) and secondary antibodies Alexa Fluor 564 (Anti-Mouse, Life Technologies, 1:2000 dilution) and Alexa Fluor 488 (Anti- Rabbit, Life Technologies, 1:2000 dilution).

Western Blotting

Mice were deeply anesthetized with ketamine (0.13 mg/g, i.p.) and xylazine (0.01 mg/g, i.p.) and cardiac perfused with (PBS). After most of the blood was cleared, brains were dissected out and sectioned at 300 μm thickness in carbogenated artificial cerebrospinal fluid (aCSF) using a vibratome. Motor cortex was isolated from these sections and homogenized in cold lysis buffer (0.5 M Tris-HCl, 150 mM NaCl, 0.1% Triton x-100, 10% sodium dexycholate, pH 6.8) with protease inhibitor (11697498001, Roche). Cell lysates were centrifuged (for 12,000 rpm for 10 min at 4°C), with the supernatants collected as samples and protein concentration determined using the Pierce BCA assay kit (Pierce, Rockford, IL). The samples were then diluted in SDS sample buffer before being heated to 100^{o}C for 5 min. Sample proteins were then separated by gel electrophoresis (7% SDS-PAGE gel, 0.04 A, 100 min) and transferred to a nitrocellulose membrane. This was then incubated with anti-KCC2 primary antibody (rabbit, 1:1000, 07-432, Millipore) and anti-βactin (mouse, 1:1000, 030M4788, Sigma-Aldrich), and secondary antibody (anti-rabbit immunoglobulin; 1:5000, HAF008, R&D systems, and anti-mouse immunoglobulins; 1:1000, HAF007, R&D systems). Protein concentration was analyzed for protein bands using ImageJ.

Electrophysiological methods

Mice were deeply anesthetised with ketamine (0.13 mg/g, i.p.) and xylazine (0.01 mg/g, i.p.) to prepared acute sections. Mice were perfused with the solution for slicing (230 sucrose, 26 NaHCO3, 2 KCl, 1 MgCl2, 1 KH2PO4, 0.5 CaCl2, 10 glucose in mM) with oxygenated (95% O2, 5% CO2). Whole brain was rapidly removed, and was cutted to coronal slices with 350 μm in thickness in cold slicing solution. Sections were placed in oxygenated artificial cerebrospinal fluid (aCSF: 124 NaCl, 3.0 KCl, 2.0 CaCl2, 25 NaHCO3, 1.1 NaH2PO4, 2.0 MgSO4, and 10 D-glucose, and was equilibrated with 95% O2 and 5% CO2 to yield a pH of 7.4 at the experimental temperature, in mM) over 1 hour before recording. Evoked inhibitory postsynaptic current (IPSC) were recorded using conventional whole-cell patch-clamp configuration with 30 μM 2-amino-5-phosphonovaleric acid (AP5) and 10μM 6-cyano-7-nitroquinoxaline-2,3-dione (CNQX). Membrane was clamped at -20 mV in recording.

Data Analysis and Statistics

Data are presented as mean ± SEM. Comparisons between control and KCC2 upregulated mice used an unpaired t-test or a one-way or two-way ANOVA, followed by a posthoc Tukey's or Bonferroni's test as indicated. Significant differences were defined by a p value of less than 0.05.

Results

Overexpression of KCC2 in Cortex. (Figure 1)

To overexpress KCC2, I utilized a conditional transgenic mouse which incorporates the tetracycline operator construct (tet-O) upstream of the KCC2 gene (Fig. 1A). Overexpression of KCC2 was driven by the expression of the tetracycline trans-activator (tTA) protein and restricted to excitatory neurons of the forebrain (cortex, hippocampus, amygdala) by coupling to the CaMKIIα promoter (Mayford et al., 1996; Sutoo et al., 2002). In mice that expressed both tet-O and tTA, overexpression of KCC2 was prevented by dietary supplementation of Dox, and triggered by cessation of Dox supplementation. Details of this transgenic mouse have been recently reported as a preprint in Goulton et al (Goulton et al., 2018), which demonstrates that Dox cessation increases KCC2 mRNA and protein expression throughout the cortex, amygdala and hippocampus. Overexpression of KCC2 does not induce obvious changes in any fundamental physiological parameters. For example, in 7-11 week old male mice without KCC2 overexpression, body weight was 25.1 ± 1.4 g (n = 13) whilst in aged matched mice with KCC2 overexpression, body weight was 27.0 ± 1.0 g (n = 11), with both values similar to the average weight of 11 weeks old male C57Bl6 mice supplied by the Jackson Laboratory (26.7 ± 1.7 g). In the current study, I first confirmed the overexpression of KCC2 protein in the motor cortex 7 days after cessation of Dox supplementation,

using Western blot experiments (Fig. 1B). The expression of KCC2 (relative to β-actin intensity) was significantly increased as compared to control mice, from 40.4 ± 9.3% (n = 3 mice) to 87.8 ± 9.8% (n = 3 mice), representing an approximate doubling of protein expression (unpaired t-test, p = 0.025; Fig. 1C). The control or wild-type (WT) mice used in this study were mice from the same colony and with the same diet, that lacked both of the two gene constructs required to induce KCC2 overexpression (tet-O, tTA).

To confirm that KCC2 overexpression was reliable across the majority of excitatory pyramidal neurons in the motor cortex, I immunostained neurons using a label against the virion protein 16 (VP16), a component of the tTA construct (Gossen and Bujard, 1992), with neurons identified by NeuN expression. As shown in Figure 1C, the majority of excitatory pyramidal neurons in layer V of the M1 motor cortex co-expressed VP16. (e.g., Fig. 1D). In four KCC2 overexpressing mice, 62 ± 3.4% of layer II/III and 69 ± 3.3% of layer V neurons that expressed NeuN also expressed VP16. Given that about 15% of these NeuN positive cells should be inhibitory neurons (Meyer et al., 2011), I estimate that withdrawal of Doxycycline would overexpress KCC2 in about 75% of all excitatory neurons. Such mosaicism for tTA/tet-O driven constructs in the absence of Dox has been previously characterized, with between 34-72% of CA1 pyramidal neurons expressing tet-O driven reporter proteins in different transgenic lines (Krestel et al., 2001).

Overexpression of KCC2 raised chloride pumping function, compared to control. (Figure 2）

Next, to examine the functional consequences of KCC2 overexpression at the membrane of excitatory neurons, I investigated the inhibitory postsynaptic response at the layer V excitatory neurons of the M1 (Fig. 2A). Previously, the difference in the amount of KCC2 expression and the potency to exclude the Cl^- out of the cells between XII (high) and DMV (low) motor neurons leads to the difference in the time course of attenuation of the amplitude of IPCSs evoked by repetitive stimulation (3.3 Hz) (Ueno et al., 2002). I recorded evoked IPSC in layer V pyramidal neurons of the M1 obtained from WT and KCC2 overexpression mice (Fig. 2A & B). During repetitive electrical stimulation applied to the inhibitory afferent to neurons recorded (5 Hz), the degree of reduction in IPSC amplitude was significantly less in KCC2 overexpression neurons than in WT neurons (WT neuron: $n = 3$, KCC2 overexpression neuron: $n = 3$, $p < 0.001$, 2-way ANOVA, Fig. C). Thus, functional of KCC2 was increased in the motor cortex of KCC2 overexpressing mice, suggesting the surface expression of KCC2 is enhanced in KCC2 overexpressing mice.

KCC2 overexpression did not affect locomotion and anxiety behaviors. （Figure 3）

I next evaluated anxiety and activity behavior, because of an increased expression of KCC2 protein level in the hippocampus, cortex and amygdala (Goulton., et al). Four groups of mice (WT with/without Dox and KCC2 with/without Dox) were used for behavioral testing (Fig. 3A). Mice

examined with open field test on day 1 were subjected to elevated plus maze test on day 2 (Fig. 3A). On open field test to assess hyperactivity and anxiety, the time to spend in 36% center area was recorded for 10 minutes (Fig. 3B, gray: anxiety area). There is no difference in time to spent in the total distance (Fig. 3D) and the anxiety area (Fig. 3E) among four groups. Elevated plus maze was employed to measure the anxiety memory (Chen et al., 2006; Han et al., 2012) (Fig. 3C, gray: anxiety area). In results, the total distance for the mice to travel was not significantly different among 4 groups (Fig. 3F). And, there was no significant differences in ratio of entry into the open arms (anxiety area, Fig. 3G). This result suggests that increasing KCC2 by withdrawing Dox for 1 week has no significant effect on basal locomotor activity and anxiety as measured in open field and elevated plus maze tests, respectively.

KCC2 overexpressing mice shows a more rapid acquisition of improved motor performance.

（Figure 4-5）

Previous studies suggest that repeated behavioral training can promote synaptic plasticity in cerebral motor cortex (Fu et al., 2012; Xu et al., 2009; Yang et al., 2009). I next assessed motor learning and memory using rotarod test. I also used different four types of mice (Fig. 4A). Single mouse was subjected to a total of 6 trials per day during successive 5 days (Fig. 4B). Each trial was composed with accelerating speeds (range, 4-40 rpm), with a maximum duration of 300 second (Fig.

4B), and an inter-trial interval of 10 min. During 5 day of training, a majority of mice gradually increased their skill of running on rotarod (Fig. 4C). Among WT, WT-Dox and KCC2-Dox mice, there was no difference in learning curve during 5 days training (WT versus WT-Dox: $p = 1.0$, WT versus KCC2-Dox: $p = 0.07$, WT-Dox versus KCC2-Dox: $p = 0.134$). While KCC2 overexpressing mice showed the more improvement of behavior than KCC2-Dox mice ($p = 0.0001$) and WT mice ($p = 0.009$), and trend to show greater (but not significant) performance compared to WT-Dox mice ($p = 0.071$) (Fig. 4C).

I examined and quantified the performance of mice during the rotarod task. I used the same mice cohort as subjected to 5 days of imaging, but also included mice in which reliable imaging across the entire protocol was unsuccessful. A series of 6 rotarod trials were performed over 5 consecutive days. Performance was measured by quantifying the time it took for mice to be no longer able to hold on to the rotarod as its speed was gradually increased in a step-wise fashion. As shown in Figure 5A, both WT and KCC2 overexpressing mice showed similar motor performance levels in the first rotarod session, and both cohorts improved in their motor performance during the 5 days of training. Nevertheless, the motor performance curves across the 5 days of training were significantly different between KCC2 overexpressing mice and WT mice (Fig, 5A; n = 15 WT mice with 6 trials per day, n= 15 KCC2 overexpressing mice with 6 trials per day, $p = 0.00095$, 2-way ANOVA with Bonferroni's test). Furthermore, the pooled motor performance from days 4 and 5 of

training was significantly better in KCC2 overexpressing mice as compared to WT mice (Fig. 5A; n = 15 WT mice, n = 15 KCC2 overexpressing mice; p = 0.0267, unpaired *t*-test). Motor performance across trials for each day were also averaged and compared to the initial motor performance level at day 1 (Fig. 5B). In WT mice, a significant improvement in performance (i.e. motor learning) was first seen at day 4 of training. Whereas for KCC2 overexpressing mice, a significant improvement in performance was first seen at day 2 of training. Thus, a significant improvement in motor performance occurred earlier in KCC2 overexpressing mice as compared to WT mice, which suggests an enhanced learning capacity. At trial 6 in both WT mice and KCC2 overexpressing mice, their performance was significantly improved, compared to trial 1 at 1st day of training. (174.6 ± 19.04 sec versus 219.73 ± 18.37 sec, p = 0.009 in WT mice; 152.87 ± 19.35 sec versus 200.60 ± 19.63 sec, p = 0.01 in KCC2 overexpression mice; paired t-test; WT: n = 15, KCC2 overexpressing: n = 15; Fig, 5C). At the 2nd day, KCC2 overexpressing mice, but not WT mice, significantly improved their behavior during the training, suggesting advanced motor efficacy (209.73 ± 18.12 sec at 1st trail versus 236.00 ± 15.53 sec at 6th trail, p = 0.13 in WT mice; 205.00 ± 19.31 sec at 1st trail versus 255.00 ± 16.87 sec at 6th trail, p = 0.007 in KCC2 overexpression mice; paired t-test; WT: n = 15, KCC2 overexpressing: n = 15; Fig, 5C). WT mice achieved significant improvement between 1st and 6th trial on 3rd day of training (216.67 ± 22.34 sec at 1st trail versus 263.00 ± 12.94 sec at 6th trail in WT mice: n = 15 Figure 5C). Hence a significant increment in performance occurred

earlier in KCC2 overexpressing mice, suggesting enhanced learning capacity.

Running activity did not change the total KCC2 protein. （Figure 6）

KCC2 expression decreases in many pathological conditions including axotomy (Nabekura et al., 2002), nerve transection (Toyoda et al., 2003) and chronic pain (Eto et al., 2012) and Oxidative stress (Wake et al., 2007), interictal-like activity (Rivera et al., 2002; Rivera et al., 2004). Motor training is supposed to facilitate the neuronal activity in the motor cortex in WT mice. Therefore, I examined the expression level of KCC2 with roratod training using western blotting method. Expression of KCC2 was examined at 15, 30, 60 and 240 minutes after single rotarod training in WT mice (Fig. 6A). There was no difference in KCC2 protein among four times (Fig. 6B & C). Next, I examined the protein level of KCC2 after 1st day and 3rd day training (Fig. 6D). Sustained repeated training did not significantly affect total KCC2 expression levels in motor cortex (Fig. 6E & F) (WT: day 1: n = 3, day 3: n = 3). Thus, the training in the present experiment did not affect the expression of KCC2 in WT mice.

Overexpression of KCC2 in mature period increased dendritic spine density of cortical layer V neurons. （Figure 7-8）

Furthermore, *in utero* overexpression of KCC2, or a transport-defective mutant KCC2,

resulted in an increase in the density of mature dendritic spines in the somatosensory cortex (Layer II/III) that was sustained for at least until 90 days after birth (Fiumelli et al., 2013). To evaluate whether increasing KCC2 in the adult brain could also increase dendritic spine density. I used in vivo two-photon imaging. Using this approach, I could also examine whether spine density changed over time. Mice were injected into motor cortical areas with the eGFP-encoding virus at mature period. Using long-term repetitive imaging, I visualized dendritic spines of layer V pyramidal neurons before and after Dox off (Fig. 7A). Dendritic spines in WT mice did not change in the density before and during 14 days after Dox off (Fig. 7B & D). In the KCC2, spine gain incrementally increased in late phase of imaging (Fig. 7C). KCC2 overexpressing mice gradually increased spine density of layer V pyramidal neurons (Fig. 7 C & D). The pooled data of spine density from days 10, 12 and 14 was significantly greater in KCC2 overexpressing mice than in WT mice ($p = 0.009$, unpaired t-test, Fig. 7E).

To obtain the base-line information of dynamics of synapse plasticity in KCC2 overexpressing mice and WT mice, I observed the generation and elimination of synapses in KCC2 overexpressing mice and WT mice. Dox was removed for Diet 3-4 weeks before imaging (Fig. 8A). Repeated imaging was performed at the interval of 2 days for 7 days (Fig. 8A, B & C). Spine formation, elimination and turnover rate were not changed throughout observation in two group (Fig. 8D, E & F). Also, each value was similar between KCC2 overexpression and WT mice. Thus, KCC2

overexpression did not affect the base-line dynamics of spines in the ordinary life of mice 5 weeks after Dox off. Because the overexpression of KCC2 increased the density of spines as shown in Fig, 7E and 8G, basal spine density in KCC2 overexpressing mice was significantly increased (≈ 40%) as compared to WT mice. Under control conditions WT mice had 0.23 ± 0.01 spines/μm (28 dendrites, 11 animals) while KCC2 overexpressing mice had 0.32 ± 0.02 spines/μm (34 dendrites, 16 animals; $p = 0.0007$; unpaired t-test). Nevertheless, my data confirms that KCC2 overexpression can increase dendritic spine density, but did not affect the spine dynamics in ordinary behavioral condition.

Overexpression of KCC2 increases spine density and the formation of new spines during motor learning.　（Figure 9）

Subjecting mice to repeated trials on an accelerating rotarod enables them to increase the time/speed before they fall off, and this motor learning has been associated with an increased formation rate of new dendritic spines specifically in layer V pyramidal neurons within the forelimb associated region of the M1 motor cortex (Xu et al., 2009). Previous studies have shown that motor learning and other forms of plasticity may be associated with modest increases in dendritic spine density (approximately 5-10% in Yang et al. (Yang et al., 2009) and Xu et al. (Xu et al., 2009)), or may be associated with no overall change depending on the balance of formation and elimination (Holtmaat and Svoboda, 2009). Under my conditions, total dendritic spine density was relatively

stable throughout 5 successive days of repeated imaging of the same dendrite, with mice undergoing rotarod training during the latter three days (see below, Fig 9A). Over the five imaging days, dendritic spine density was consistently higher in KCC2 overexpressing mice (by 30-40%) across each of these days (Fig. 9B-D). When images of dendrites and their spines were compared between two consecutive days, a significant increase in the proportion of newly appeared dendritic spines (dendritic spine formation rate) was seen in mice overexpressing KCC2 following a single day of rotarod training (Fig. 3B-C, 3E). Between the two pre-training control days (day -1 to day 0), the dendritic spine formation rate in KCC2 overexpressing mice was 6.94 ± 1.11%, whereas after one day of training the dendritic spine formation rate increased to 13.49 ± 1.58% (day 0 to day 1, 23 dendrites, 7 animals, one-way ANOVA, Tukey's test, $p = 0.036$, Fig. 9E). The corresponding rates of new dendritic spine formation pre and post 1 day training in WT mice was 5.28 ± 1.52% and 12.00 ± 1.57% (18 dendrites, 7 animals; one-way ANOVA, Tukey's test, not significantly different, Fig. 3E). In both WT and KCC2 overexpressing mice the proportion of dendritic spines that disappeared across consecutive imaging days (dendritic spine elimination rate) was relatively constant across the 5 days of imaging (between 5-10%) and not significantly different between WT and KCC2 overexpressing mice (Fig. 3F). Corresponding with the increased dendritic spine formation in KCC2 overexpressing mice, the dendritic spine turnover rate (an average of elimination and formation) seen after 1 day of training was also significantly increased in KCC2 overexpressing mice (11.45 ±

1.13; one-way ANOVA, Tukey's test, p = 0.0097; Fig. 3G), but not in WT mice (6.76 ± 0.98%).

Stability of newly formed and existing dendritic spines. (Figure 10)

Most newly formed spines are labile and are eliminated over the subsequent weeks. However, a proportion of spines that are newly formed during learning of a specific motor task, such as accelerating rotarod training or forelimb reaching, persist for a longer time suggesting they help encode the storage of that learning information (Xu et al., 2009; Yang et al., 2009). In addition, training can enhance the elimination of existing spines (Yang et al., 2009). Hence, I next examined the stability of existing and newly formed spines. Although the absolute and relative numbers of new spines seen in KCC2 overexpressing mice was greater than in WT mice (Fig. 9E), these new spines were similarly labile and both WT and KCC2 overexpressing mice had similar rates of elimination of spines that existed prior to the rotarod training (Fig. 10A & B). I then examined the stability of spines that newly formed over the first 2 days of training (Fig. 10C & D). In both WT and KCC2 overexpressing mice, approximately 20% of the new spines seen after 1 or 2 days of rotarod training had disappeared by about 24 hrs later. However, survival number of new spines generated at 1st day was significant greater from day 1 to day 2 in KCC2 overexpressing mice compared with that in WT mice (Fig. 10E). But there was less difference in survival number at 3rd day of new spines generated at 2nd day (Fig. 10E). Thus, increased number of new spines, not their turn-over, might be important

for improvement of performance.

Increasing number of new spine formation facilitates the behavioral improvement in following day. (Figure 11)

Next, to gain understanding of the functional importance of newly formed spines, I examined the correlation between the survival rate of newly generated spines and behavioral performance as previously reports (Xu et al., 2009; Yang et al., 2009). I investigated the relationship between the rate of newly generated spines and the improvement of motor behavior. In WT mice, the percentage of newly formed spines are significantly correlated with improvement performance during 1st day of training ($p = 0.01$, $r = 0.87$; Fig. 11A), but not at 2nd day (Fig. 11B). Interestingly, the newly formed spines at the 1st day of training tend to be correlated, although it is not significant, with the improvement of motor skill during 2nd day of training ($p = 0.07$, $r = 0.7$; Fig. 11C). This result suggests that motor training increased the number of new spines which is correlated with the improvement of motor skill. In addition, surplus formation of the spines, in case of KCC2 overexpressing mice, also affects the motor learning in the following day.

Up-regulating of KCC2 promotes synaptic plasticity and motor skill. （Figure 12）

In the present study, I examined the possibility that the enhancement of KCC2 facilitate the

training-dependent synaptic plasticity in the motor cortex and learning ability. Using a conditional transgenic mouse strategy, I examined whether overexpression of KCC2 enhances dendritic spines in the adult nervous system, and characterized the effects on spine dynamics in the motor cortex *in vivo* during rotarod training. Mice overexpressing KCC2 showed significantly increased spine density in the apical dendrites of layer V pyramidal neurons, measured *in vivo* using two photon imaging (Fig. 12A, upper). During modest accelerated rotarod training, mice overexpressing KCC2 displayed enhanced spine formation rates, greater balancing skill at higher rotarod speeds and a faster rate of learning in this ability (Fig. 12A, bottom). My results demonstrate that KCC2 enhances spine density and dynamics in the adult nervous system and suggests that KCC2 may play a role in experience-dependent synaptic plasticity.

Discussion

Using a conditional transgenic mouse where KCC2 is overexpressed in excitatory pyramidal neurons by ceasing dietary doxycycline supplementation I have shown that: 1) increasing KCC2 in the brain after the major developmental period of synaptogenesis can increase dendritic spine density, 2) that increasing KCC2 enhances the capacity of motor learning to form new dendritic spines, and 3) increasing KCC2 increases the extent and rate of performance increase during training. Hence my data strongly supports the growing appreciation of the role of KCC2 in dendritic spine development, maturation and/or maintenance, and extends this to a putative role in enhancing synaptic plasticity and performance during learning *in vivo*.

In-utero transfection of KCC2 into cortex results in a permanent increase in dendritic spine density of between 50-100% when measured at different postnatal times and in different regions of layer II/III neurons. For example, in apical and basal dendrites from mice at 3 months of age, spine density was approximately 90% higher (Fiumelli et al., 2013). This increase in dendritic spines was supported by an approximately 70% increase in the frequency of miniature excitatory postsynaptic currents (mEPSCs; at postnatal day 30-34; (Fiumelli et al., 2013)). Conversely, neurons cultured from KCC2 knockout mice, showed an approximate halving of synapses identified by both glutamate transporter (VGLUT) staining and by mEPSC frequency (Li et al., 2007). It has been debated whether these striking effects of KCC2 on synapse numbers may be at least partly due to an

impact on developmental spinogenesis. Knocking down KCC2 in more mature hippocampal cultures has not been associated with significant changes in dendritic spine density or mEPSC frequency, although knocking out KCC2 in developing neuronal cultures did alter dendritic spine volume, AMPA receptor aggregation and quantal size (Gauvain et al., 2011). My present results show that overexpressing KCC2 in the postnatal brain *in vivo* lead to a significant increase in dendritic spine density in hippocampus and motor cortex (but not somatosensory cortex). However, the extent of this increase in the motor cortex was 40-50% less than that achieved when KCC2 was manipulated prior to spinogenesis in development (Awad et al., 2016; Fiumelli et al., 2013). While two reports have shown that shRNA induced knockdown of KCC2 decreases hippocampal dendritic spine density (Llano et al., 2015), a more recent report demonstrated that overexpression of KCC2 decreases dendritic spine density in CA1 neurons, both *in vivo* and in organotypic slice cultures . In the same study, dendritic spine density was increased in pyramidal neurons of the cortex after KCC2 overexpression, indicating regional differences (Awad et al., 2018). The effects of KCC2 on dendritic spine density may depend on the extent of effects of KCC2 on spinogenesis and on neuronal excitability, which may further relate to regional and age-dependent differences in relative membrane levels of KCC2 and on other neuroactive molecules such as brain-derived neurotrophic factor (Awad et al., 2018). It will be important to also determine if adult KCC2 expression is associated with an increased dendritic spine head diameter and the number of functional excitatory

synapses, as has been observed with in utero electroporation of KCC2 (Fiumelli et al., 2013). In the present study, whilst I did not specifically compare the morphology of dendritic spines nor the number of functional synapses, the elimination rates of the dendritic spines in KCC2 overexpressing and WT mice over the 3 day imaging period were similar which suggests that the additional dendritic spines in KCC2 overexpressing mice could be similar to mature dendritic spines in WT mice.

Experience dependent changes in dendritic spine number, size and spatial arrangements are important components of structural synaptic plasticity that accompanies learning and memory formation (Fu and Zuo, 2011; Lu and Zuo, 2017). In the adult brain, most dendritic spines are generally very stable with a small proportion (≈ 5%) being continuously formed and eliminated. Learning can increase this new dendritic spine formation rate and promote elimination of pre-existing dendritic spines. Motor training on an accelerated rotarod, for example, causes an approximate 5% increase in dendritic spine formation in the forelimb area of the motor cortex in adult mice (Yang et al., 2009). Similar increases in dendritic spine formation rates are seen in other motor tasks, such as learning to reach for a pellet (Tjia et al., 2017; Xu et al., 2009). The extent of the increase in formation rate can depend on many factors including age, specific cortical layer and dendritic branch, as well as sleep and glucocorticoid status (Liston et al., 2013; Tjia et al., 2017; Yang et al., 2014). Some of the newly formed dendritic spines persist, with the degree of dendritic

spine stability correlated with the degree of learning (Xu et al., 2009). In my current study, I used a more modest rotarod training regime and did not detect significant increases in dendritic spine formation rates in WT mice, nor did I detect correlations between the extent of performance increments and new dendritic spine formation or stability, as has been previously reported in Yang et al. (Yang et al., 2009) and Liston et al. (Liston et al., 2013). My rotarod accelerated to a maximum of 40 rpm and I trained with 6 trials per session (for 5 days) whereas Yang et al. (Yang et al., 2009) for example, accelerated to 100 rpm and trained with 20 trials per session (for 2 days). Despite this modest training protocol, I still observed a significant increase in dendritic spine formation rate in mice overexpressing KCC2. Hence, as well as increasing basal spine levels, KCC2 overexpression may facilitate the capacity for motor training to form new dendritic spines. Related to this, KCC2 overexpression was also associated with subtle yet significant increases in the rate and extent of performance increase resulting from the rotarod training. I speculate that the significant increase in performance seen at day 2 in the KCC2 overexpressing mice may be related to the increase in dendritic spine formation seen following training on day 1, enabling at least part of the structural component of synapses to be more readily available to encode the learning associated with subsequent training. Indeed, daily significant increments in motor performance improvement and dendritic spine formation were only seen on all days of the training protocol in KCC2 overexpressing mice. This assumes that the locus of the rotarod learning resides in the motor cortex,

although other regions related to motor activity, e.g. thalamus and cerebellum, may be affected by KCC2 and also be involved in the motor performance changes. Clearly KCC2 overexpression will also affect Cl^- homeostasis, GABAergic inhibition and neuronal excitability and I am as yet unable to distinguish the aspects of enhanced behavioral learning that are solely attributable to the dendritic spine effects. Transport deficient KCC2 mutations may be able to probe this, as described in Li et al. (Li et al., 2007), Fiumelli et al. (Fiumelli et al., 2013), but see Awad et al.(Awad et al., 2018). Nevertheless, my tantalizing results raise the possibility that KCC2 may be involved in synaptic plasticity in the adult nervous system and should encourage further studies to more closely examine this hypothesis.

Acknowledgements

I would like to give my heartfelt appreciation Professor Junichi Nabekura for supervising the experiments.

I would like to thank associate professor Moorhouse, Andrew John and Dennis Lawrence at School of Medical Sciences, University of New South Wales, Sydney, during the review process are highly appreciated. I also thank to Dr. Kei Eto for teaching electrophysiology experiment. I thank Ms. Tatsuko Oba for the support of animal maintenance and preparation, also Dr. Miho Watanabe at Hamamatsu Medical University for a useful suggestion for the analysis of KCC2 expression and staining.

I am also indebted all member of laboratory of the division of Homeostatic Development and National Institute for Physiological Science for their supports and inspiring discussion.

References

1. Awad, P.N., Amegandjin, C.A., Szczurkowska, J., Carriço, J.N., Fernandes do Nascimento, A.S., Baho, E., Chattopadhyaya, B., Cancedda, L., Carmant, L., and Di Cristo, G. (2018). KCC2 Regulates Dendritic Spine Formation in a Brain-Region Specific and BDNF Dependent Manner. Cerebral Cortex *28*, 4049-4062.
2. Awad, P.N., Sanon, N.T., Chattopadhyaya, B., Carriço, J.N., Ouardouz, M., Gagné, J., Duss, S., Wolf, D., Desgent, S., Cancedda, L.*, et al.* (2016). Reducing premature KCC2 expression rescues seizure susceptibility and spine morphology in atypical febrile seizures. Neurobiology of Disease *91*, 10-20.
3. Bosch, M., and Hayashi, Y. (2012). Structural plasticity of dendritic spines. Current opinion in neurobiology *22*, 383-388.
4. Chamma, I., Heubl, M., Chevy, Q., Renner, M., Moutkine, I., Eugene, E., Poncer, J.C., and Levi, S. (2013). Activity-dependent regulation of the K/Cl transporter KCC2 membrane diffusion, clustering, and function in hippocampal neurons. J Neurosci *33*, 15488-15503.
5. Chen, Z.Y., Jing, D., Bath, K.G., Ieraci, A., Khan, T., Siao, C.J., Herrera, D.G., Toth, M., Yang, C., McEwen, B.S.*, et al.* (2006). Genetic variant BDNF (Val66Met) polymorphism alters anxiety-related behavior. Science *314*, 140-143.
6. Chevy, Q., Heubl, M., Goutierre, M., Backer, S., Moutkine, I., Eugene, E., Bloch-Gallego, E., Levi, S., and Poncer, J.C. (2015). KCC2 Gates Activity-Driven AMPA Receptor Traffic through Cofilin Phosphorylation. The Journal of neuroscience : the official journal of the Society for Neuroscience *35*, 15772-15786.
7. Delpire, E. (2000). Cation-Chloride Cotransporters in Neuronal Communication. News in physiological sciences : an international journal of physiology produced jointly by the International Union of Physiological Sciences and the American Physiological Society *15*, 309-312.
8. Eto, K., Ishibashi, H., Yoshimura, T., Watanabe, M., Miyamoto, A., Ikenaka, K., Moorhouse, A.J., and Nabekura, J. (2012). Enhanced GABAergic activity in the mouse primary somatosensory cortex is insufficient to alleviate chronic pain behavior with reduced expression of neuronal potassium-chloride cotransporter. The Journal of neuroscience : the official journal of the Society for Neuroscience *32*, 16552-16559.
9. Fiumelli, H., Briner, A., Puskarjov, M., Blaesse, P., Belem, B.J., Dayer, A.G., Kaila, K., Martin, J.L., and Vutskits, L. (2013). An ion transport-independent role for the cation-chloride cotransporter KCC2 in dendritic spinogenesis in vivo. Cerebral cortex *23*, 378-388.
10. Fu, M., Yu, X., Lu, J., and Zuo, Y. (2012). Repetitive motor learning induces coordinated formation of clustered dendritic spines in vivo. Nature *483*, 92-95.

11. Fu, M., and Zuo, Y. (2011). Experience-dependent structural plasticity in the cortex. Trends in Neurosciences *34*, 177-187.
12. Gauvain, G., Chamma, I., Chevy, Q., Cabezas, C., Irinopoulou, T., Bodrug, N., Carnaud, M., Lévi, S., and Poncer, J.C. (2011). The neuronal K-Cl cotransporter KCC2 influences postsynaptic AMPA receptor content and lateral diffusion in dendritic spines. Proceedings of the National Academy of Sciences of the United States of America *108*, 15474-15479.
13. Gossen, M., and Bujard, H. (1992). Tight control of gene expression in mammalian cells by tetracycline-responsive promoters. Proceedings of the National Academy of Sciences of the United States of America *89*, 5547-5551.
14. Goulton CS, Watanabe M, Cheung DL, Wang KW, Oba T, Khoshaba A, Lai D, Inada H, Eto K, Nakamura K, Power JM, Lewis TM, Housley GD, Wake H, Nabekura J, and Moorhouse AJ (2018) Conditional upregulation of KCC2 selectively enhances neuronal inhibition during seizures. bioRxiv. *10*.1101/253831 %J bioRxiv
15. Gulyas, A.I., Sik, A., Payne, J.A., Kaila, K., and Freund, T.F. (2001). The KCl cotransporter, KCC2, is highly expressed in the vicinity of excitatory synapses in the rat hippocampus. Eur J Neurosci *13*, 2205-2217.
16. Han, S., Tai, C., Westenbroek, R.E., Yu, F.H., Cheah, C.S., Potter, G.B., Rubenstein, J.L., Scheuer, T., de la Iglesia, H.O., and Catterall, W.A. (2012). Autistic-like behaviour in Scn1a+/- mice and rescue by enhanced GABA-mediated neurotransmission. Nature *489*, 385-390.
17. Holtmaat, A., and Svoboda, K. (2009). Experience-dependent structural synaptic plasticity in the mammalian brain. Nat Rev Neurosci *10*, 647-658.
18. Kaila, K. (1994). Ionic basis of GABAA receptor channel function in the nervous system. Progress in neurobiology *42*, 489-537.
19. Kakazu, Y., Akaike, N., Komiyama, S., and Nabekura, J. (1999). Regulation of intracellular chloride by cotransporters in developing lateral superior olive neurons. The Journal of neuroscience : the official journal of the Society for Neuroscience *19*, 2843-2851.
20. Kakegawa, W., Miyoshi, Y., Hamase, K., Matsuda, S., Matsuda, K., Kohda, K., Emi, K., Motohashi, J., Konno, R., Zaitsu, K.*, et al.* (2011). D-serine regulates cerebellar LTD and motor coordination through the delta2 glutamate receptor. Nat Neurosci *14*, 603-611.
21. Kasai, H., Fukuda, M., Watanabe, S., Hayashi-Takagi, A., and Noguchi, J. (2010). Structural dynamics of dendritic spines in memory and cognition. Trends Neurosci *33*, 121-129.
22. Kim, S.K., Hayashi, H., Ishikawa, T., Shibata, K., Shigetomi, E., Shinozaki, Y., Inada, H., Roh, S.E., Kim, S.J., Lee, G.*, et al.* (2016). Cortical astrocytes rewire somatosensory cortical circuits for peripheral neuropathic pain. J Clin Invest *126*, 1983-1997.
23. Kim, S.K., and Nabekura, J. (2011). Rapid synaptic remodeling in the adult somatosensory cortex following peripheral nerve injury and its association with neuropathic pain. J Neurosci *31*,

5477-5482.

24. Krestel, H.E., Mayford, M., Seeburg, P.H., and Sprengel, R. (2001). A GFP-equipped bidirectional expression module well suited for monitoring tetracycline-regulated gene expression in mouse. Nucleic acids research *29*, E39-E39.
25. Lee, H.H., Walker, J.A., Williams, J.R., Goodier, R.J., Payne, J.A., and Moss, S.J. (2007). Direct protein kinase C-dependent phosphorylation regulates the cell surface stability and activity of the potassium chloride cotransporter KCC2. The Journal of biological chemistry *282*, 29777-29784.
26. Li, H., Khirug, S., Cai, C., Ludwig, A., Blaesse, P., Kolikova, J., Afzalov, R., Coleman, S.K., Lauri, S., Airaksinen, M.S.*, et al.* (2007). KCC2 Interacts with the Dendritic Cytoskeleton to Promote Spine Development. Neuron *56*, 1019-1033.
27. Liston, C., Cichon, J.M., Jeanneteau, F., Jia, Z., Chao, M.V., and Gan, W.-B. (2013). Circadian glucocorticoid oscillations promote learning-dependent synapse formation and maintenance. Nature Neuroscience *16*, 698.
28. Llano, O., Smirnov, S., Soni, S., Golubtsov, A., Guillemin, I., Hotulainen, P., Medina, I., Nothwang, H.G., Rivera, C., and Ludwig, A. (2015). KCC2 regulates actin dynamics in dendritic spines via interaction with β-PIX. J Cell Biology *209*, 671-686.
29. Lu, J., and Zuo, Y. (2017). A Local Rebalancing Act Leads to Global Benefit. Neuron *96*, 712-713.
30. Ludwig, A., Li, H., Saarma, M., Kaila, K., and Rivera, C. (2003). Developmental up-regulation of KCC2 in the absence of GABAergic and glutamatergic transmission. The European journal of neuroscience *18*, 3199-3206.
31. Mayford, M., Bach, M.E., Huang, Y.Y., Wang, L., Hawkins, R.D., and Kandel, E.R. (1996). Control of memory formation through regulated expression of a CaMKII transgene. Science *274*, 1678-1683.
32. Meyer, H.S., Schwarz, D., Wimmer, V.C., Schmitt, A.C., Kerr, J.N.D., Sakmann, B., and Helmstaedter, M. (2011). Inhibitory interneurons in a cortical column form hot zones of inhibition in layers 2 and 5A. *108*, 16807-16812.
33. Nabekura, J., Ueno, T., Okabe, A., Furuta, A., Iwaki, T., Shimizu-Okabe, C., Fukuda, A., and Akaike, N. (2002). Reduction of KCC2 expression and GABAA receptor-mediated excitation after in vivo axonal injury. The Journal of neuroscience : the official journal of the Society for Neuroscience *22*, 4412-4417.
34. Penzes, P. (2007). Pumping up the synapse. Neuron *56*, 942-944.
35. Rivera, C., Li, H., Thomas-Crusells, J., Lahtinen, H., Viitanen, T., Nanobashvili, A., Kokaia, Z., Airaksinen, M.S., Voipio, J., Kaila, K.*, et al.* (2002). BDNF-induced TrkB activation down-regulates the K+-Cl- cotransporter KCC2 and impairs neuronal Cl- extrusion. The Journal of cell biology *159*, 747-752.
36. Rivera, C., Voipio, J., Payne, J.A., Ruusuvuori, E., Lahtinen, H., Lamsa, K., Pirvola, U., Saarma, M., and Kaila, K. (1999). The K+/Cl- co-transporter KCC2 renders GABA hyperpolarizing during

neuronal maturation. Nature *397*, 251-255.

37. Rivera, C., Voipio, J., Thomas-Crusells, J., Li, H., Emri, Z., Sipila, S., Payne, J.A., Minichiello, L., Saarma, M., and Kaila, K. (2004). Mechanism of activity-dependent downregulation of the neuron-specific K-Cl cotransporter KCC2. The Journal of neuroscience : the official journal of the Society for Neuroscience *24*, 4683-4691.
38. Rothwell, P.E., Fuccillo, M.V., Maxeiner, S., Hayton, S.J., Gokce, O., Lim, B.K., Fowler, S.C., Malenka, R.C., and Sudhof, T.C. (2014). Autism-associated neuroligin-3 mutations commonly impair striatal circuits to boost repetitive behaviors. Cell *158*, 198-212.
39. Sutoo, D., Akiyama, K., and Yabe, K. (2002). Comparison analysis of distributions of tyrosine hydroxylase, calmodulin and calcium/calmodulin-dependent protein kinase II in a triple stained slice of rat brain. Brain Res *933*, 1-11.
40. Tjia, M., Yu, X., Jammu, L.S., Lu, J., and Zuo, Y. (2017). Pyramidal Neurons in Different Cortical Layers Exhibit Distinct Dynamics and Plasticity of Apical Dendritic Spines. Front Neural Circuits *11*.
41. Toyoda, H., Ohno, K., Yamada, J., Ikeda, M., Okabe, A., Sato, K., Hashimoto, K., and Fukuda, A. (2003). Induction of NMDA and GABAA receptor-mediated Ca2+ oscillations with KCC2 mRNA downregulation in injured facial motoneurons. Journal of neurophysiology *89*, 1353-1362.
42. Ueno, T., Okabe, A., Akaike, N., Fukuda, A., and Nabekura, J. (2002). Diversity of neuron-specific K+-Cl- cotransporter expression and inhibitory postsynaptic potential depression in rat motoneurons. The Journal of biological chemistry *277*, 4945-4950.
43. Wake, H., Moorhouse, A.J., Jinno, S., Kohsaka, S., and Nabekura, J. (2009). Resting microglia directly monitor the functional state of synapses in vivo and determine the fate of ischemic terminals. J Neurosci *29*, 3974-3980.
44. Wake, H., Watanabe, M., Moorhouse, A.J., Kanematsu, T., Horibe, S., Matsukawa, N., Asai, K., Ojika, K., Hirata, M., and Nabekura, J. (2007). Early changes in KCC2 phosphorylation in response to neuronal stress result in functional downregulation. The Journal of neuroscience : the official journal of the Society for Neuroscience *27*, 1642-1650.
45. Xu, T., Yu, X., Perlik, A.J., Tobin, W.F., Zweig, J.A., Tennant, K., Jones, T., and Zuo, Y. (2009). Rapid formation and selective stabilization of synapses for enduring motor memories. Nature *462*, 915-919.
46. Yang, G., Lai, C.S.W., Cichon, J., Ma, L., Li, W., and Gan, W.-B. (2014). Sleep promotes branch-specific formation of dendritic spines after learning. Science *344*, 1173-1178.
47. Yang, G., Pan, F., and Gan, W.B. (2009). Stably maintained dendritic spines are associated with lifelong memories. Nature *462*, 920-924.
48. Yu, X., and Zuo, Y. (2011). Spine plasticity in the motor cortex. Curr Opin Neurobiol *21*, 169-174.

Figures and Figure legends

Figure 1. Overexpression of KCC2 was induced in the cerebral cortex including the M1 by discontinuation of oral administration of doxycycline.

A. Overexpression of KCC2 was driven by the expression of the tetracycline trans-activator (tTA) protein and restricted to excitatory neurons of the forebrain (cortex, hippocampus, amygdala) by coupling to the CaMKIIα promoter.

B. Representative Western blots for KCC2 immunoreactivity in tissue from the motor cortex obtained from three WT (left) and KCC2 overexpressing (right) mice. Samples were obtained from mice 7 days after withdrawal of Doxycycline (Dox) from the diet, to induce overexpression in KCC2 mice.

C. Quantification of the intensity of KCC2 immunoreactivity, expressed relative to β-actin. The relative expression of KCC2 was significantly greater in KCC2 overexpressing mice as compared to WT mice, with the absolute KCC2/β-actin ratios being 40.4 ± 9.3% for WT (n = 3) and 87.8 ± 9.8% for KCC2 mice (n = 3; unpaired t-test,*$p < 0.05$). This corresponded to a 117% increase in KCC2 protein expression levels.

D. Representative immunohistochemical images of a brain slice from a KCC2 overexpressing transgenic mouse showing the primary motor cortex (left) stained positive for NeuN (red, neuronal marker) and VP16 (green, marker for the tetO-KCC2 construct). Most larger layer V

pyramidal neurons were double-labelled (yellow). Bar; 500 μm (left), 10 μm (upper right) and 50 μm (bottom right).

Figure 1

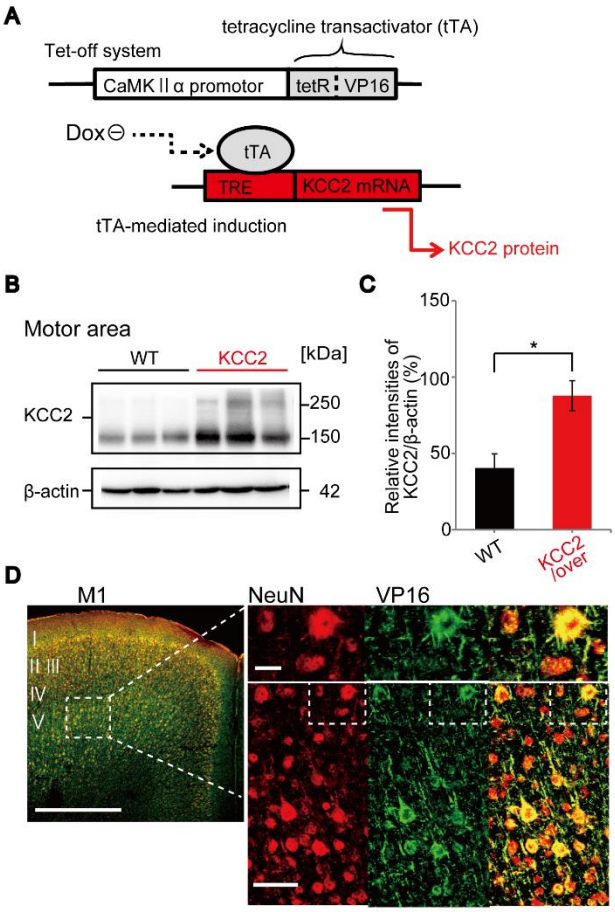
A
tetracycline transactivator (tTA)
Tet-off system
CaMK II α promotor
tetR VP16
Dox⊖
tTA
TRE
KCC2 mRNA
tTA-mediated induction
KCC2 protein
B
Motor area
WT
KCC2
[kDa]
KCC2
250
150
β-actin
42
C
Relative intensities of KCC2/β-actin (%)
150
100
50
0
*
WT
KCC2 over
D
M1
NeuN
VP16
I
II III
IV
V

Figure 2. Overexpression of KCC2 raised chloride pumping function, compared to control.

A. Actual representative image (Left). Schematic drawing of miniature IPSC recording and the electrical stimulation of Layer II/III and Layer V (right).

B. The amplitudes of IPSC greatly decreased during stimulation both in WT neuron (Black line) and KCC2 overexpression neuron (Red line).

C. Relative amplitude of each response was analysis as a ratio to that of the first IPSC during stimulation. Decreased amplitudes of IPSC more less in KCC2 overexpression neurons ($n = 3$) during stimulation, compared to WT neurons ($n = 3$, $^{***}p < 0.001$, 2-way ANOVA) .

Figure 2

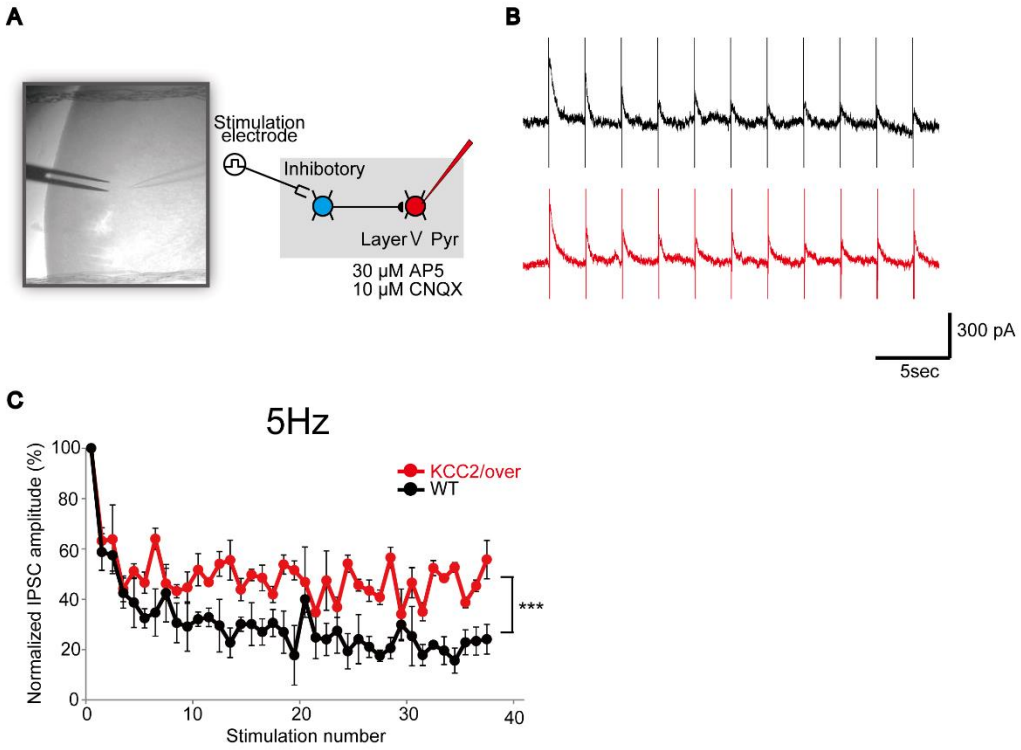
A
Stimulation electrode
Inhibotory
Layer V Pyr
30 μM AP5
10 μM CNQX
B
300 pA
5sec
C
5Hz
KCC2/over
WT
Normalized IPSC amplitude (%)
100
80
60
40
20
0
0
10
20
30
40
Stimulation number
***

Figure 3. KCC2 expression was not effect on locomotion and anxiety behaviours.

Four groups of mice (WT with/without Dox and KCC2 with/without Dox) were used for behavioral testing. KCC2-Dox (black square; n = 9), control WT-Dox (black triangle; n = 8), or no with doxycycline WT (black cyclic; n = 8) and KCC2 overexpressing mice (red cyclic; n = 8).

A. Diagram of the open field test and elevated plus maze testing protocol. The mouse performed the open field test on the 1 day, and conducted the elevated plus maze test on the 2 day.

B. The open field box comprised with equal sides of 40 cm, and the centre area (24 x 24 cm) consisted 36% of the total field area (gray area).

C. The elevated plus maze comprised an elevated (50 cm) maze structure of arms (60 cm each). Two of the arms consisted without walls (gray area), addition the other two arms had 10 cm walls around them.

D. Total distance moved during 10 mins in an open field.

E. Rate of the time moved in the centre area during 10 mins in the open field.

F. Total distance travelled during 10 minutes in the elevated plus maze test.

G. Proportion of the time spent in the open arms during 5 minutes in the elevated plus maze test.

2-way ANOVA, Bonferroni's. Data are shown as means ± SEM.

Figure 3

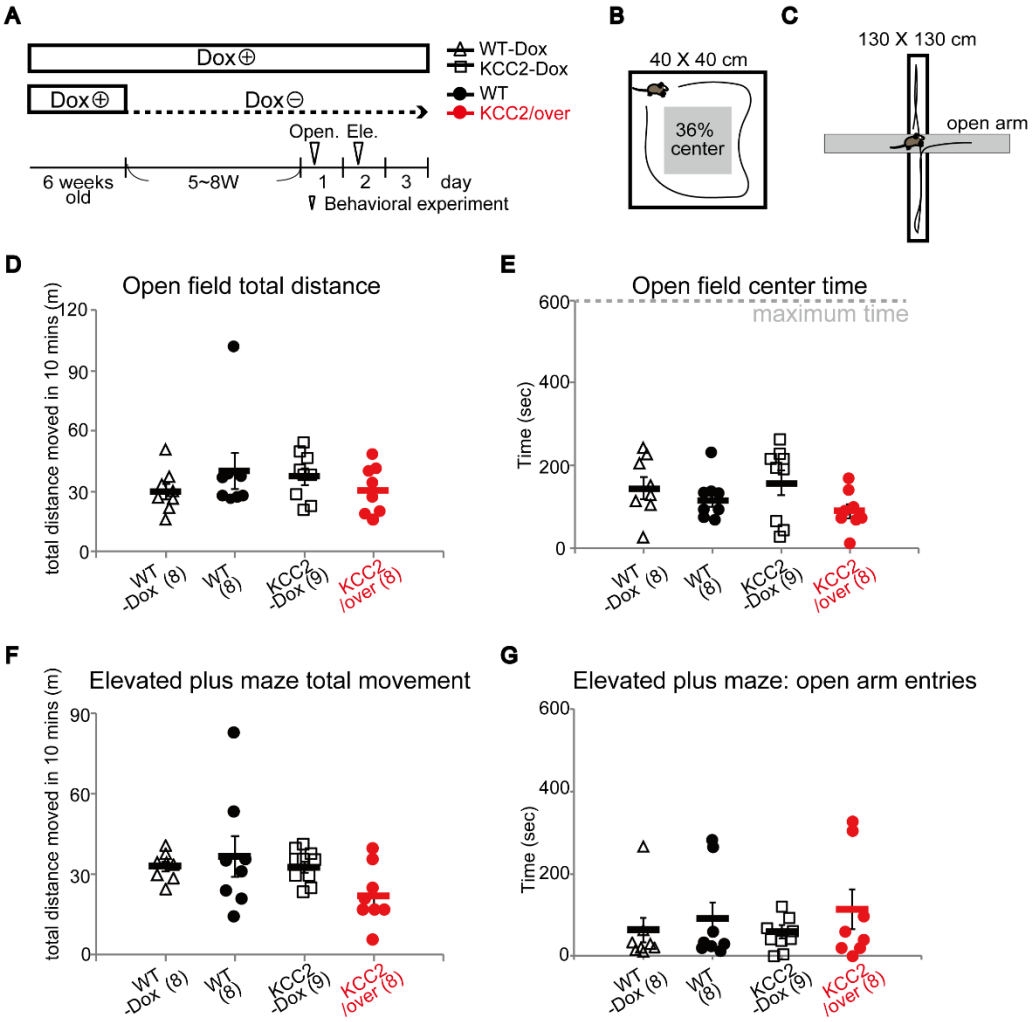
A
Dox⊕
Dox⊕
Dox⊖
WT-Dox
KCC2-Dox
WT
KCC2/over
Open. Ele.
6 weeks old
5~8W
1
2
3
day
Behavioral experiment
B
40 X 40 cm
36% center
C
130 X 130 cm
open arm
D
Open field total distance
total distance moved in 10 mins (m)
120
90
60
30
0
WT -Dox (8)
WT (8)
KCC2 -Dox (9)
KCC2 /over (8)
E
Open field center time
maximum time
Time (sec)
600
400
200
0
F
Elevated plus maze total movement
G
Elevated plus maze: open arm entries

Figure 4. Overexpression of KCC2 improves motor skill learning *in vivo*.

Mice were exposed to the motor learning task while receiving KCC2-Dox (black square; n = 6), control WT-Dox (black triangle; n = 7), or no with doxycycline WT (black cyclic; n = 15) and KCC2 overexpressing mice (red cyclic; n = 15).

A. Experimental timeline. Motor learning was performed 3 weeks after the cease of oral administration of doxycycline in mice.

B. The test was carried out one daily session consisting of 6 trials separated by at least a 10 min interval (right). The speed of the rod (r.p.m) was set to accelerate from 4 to 40 rpm over a 300 second period (left).

C. Motor learning acquisition in 5 day shown as the time to fall off from rod. KCC2 overexpressing mice show significantly improved motor learning compared with WT (**p < 0.01, 2-way ANOVA, Bonferroni's), and KCC2-Dox (***p < 0.001, 2-way ANOVA, Bonferroni's). No significant difference was observed between WT-Dox, WT and KCC2-Dox.

Figure 4

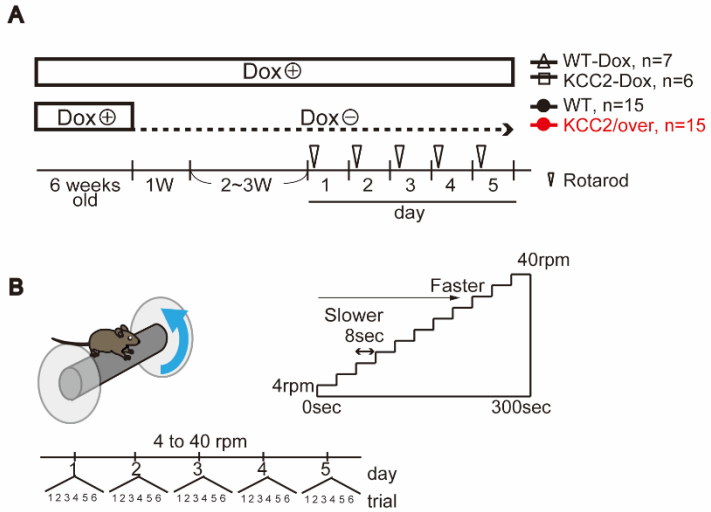
A
Dox⊕
Dox⊕
Dox⊖
WT-Dox, n=7
KCC2-Dox, n=6
WT, n=15
KCC2/over, n=15
6 weeks old
1W
2~3W
1
2
3
4
5
day
Rotarod
B
40rpm
Faster
Slower
8sec
4rpm
0sec
300sec
4 to 40 rpm
1
2
3
4
5
day
1 2 3 4 5 6
trial
C
WT-Dox
KCC2-Dox
WT
KCC2/over
Time to fall off (sec)
400
300
200
100
0
1
2
3
4
5
day
KCC2/over
WT-Dox
WT
KCC2-Dox
n.s.
**
***

Figure 5. KCC2 overexpressing mice achieved more efficiently learning, compared with WT mice.

Following withdrawal of Dox for 2-3 weeks, mice underwent 6 trials of accelerating rotarod training per day over 5 successive days (WT mice: black; n = 15; KCC2 overexpressing mice: red; n = 15).

A. Rotarod performance was measured as the time before falling off as rotarod was accelerated from 4 to 40 rpm over 300 seconds in each trial. The improvement of performance during the successive 5 day training sessions was significantly greater in KCC2 overexpressing mice as compared with WT mice (***$p < 0.001$, 2-way ANOVA with Bonferroni's test).

B. Comparison of the increase in rotarod performance across each day of training in WT (left, black) and KCC2 overexpressing mice (right, red). The performance in each of the 6 trials was averaged for each day, and the averaged performance compared to that on day 1 to evaluate the time course of the motor learning. For WT mice a significant improvement was seen by day 4 (n = 15, *$p < 0.05$, one-way ANOVA, Bonferroni's test), while for KCC2 overexpressing mice, a significant increase in performance was seen earlier, on the 2nd day of training (n = 15, *$p < 0.05$, ***$p < 0.001$, one-way ANOVA, Bonferroni's test). Data are shown as means ± SEM.

C. In each day, significant improvement of motor skill is evident, compared between 1st and last (6th) trial, at 1st and 2nd day in KCC2 overexpressing mice (n = 15), while it is not apparent at 2nd day, but evident at 3rd day, in the WT mice (n = 15, *$p < 0.05$, **$p < 0.01$, paired t-test).

Figure 5

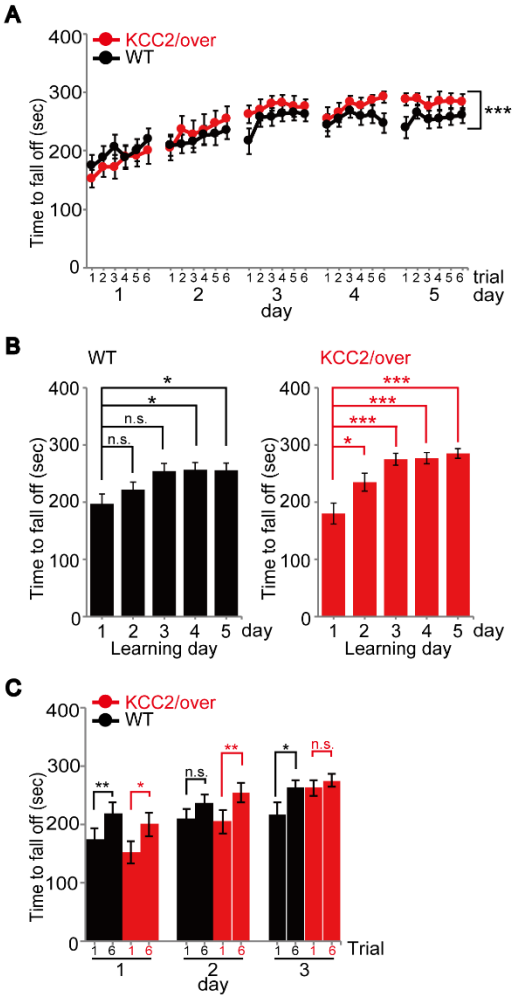
A
KCC2/over
WT
Time to fall off (sec)
400
300
200
100
0
***
1 2 3 4 5 6
trial
1
2
3
day
4
5
day
B
WT
KCC2/over
*
n.s.
***
Time to fall off (sec)
1 2 3 4 5 day
Learning day
C
KCC2/over
WT
**
n.s.
Trial
1
2
day
3

Figure 6. Running activity not led to a changed amount of total KCC2 protein.

A. Experimental timeline. KCC2 protein expression early confirmed after rotarod running of WT mice.

B. Western blots shown total KCC2 expression in M1 including forelimb area, before rotarod (control) and 15-240 mins after training. The top band show KCC2 protein (~ 150 kDa band), the bottom shown expression levels of βactin as a control, prepared from the same slice.

C. Statistical representation of optical densities of total KCC2 protein level from WT animals, expressed as percentage of control (means ± SEM).

D. Experimental timeline. KCC2 protein expression confirmed on day 1 and day 3 after rotarod running of WT mice.

E. Western blots of KCC2 protein (top panel) and actin protein (bottom panel) at day 1 and day 3 after rotarod, expressed in control conditions.

F. Averaged ratio of optical density of total KCC2 against control show at day1 and day3. Each bar represents the mean and SEM of data from each three animals.

Figure 6

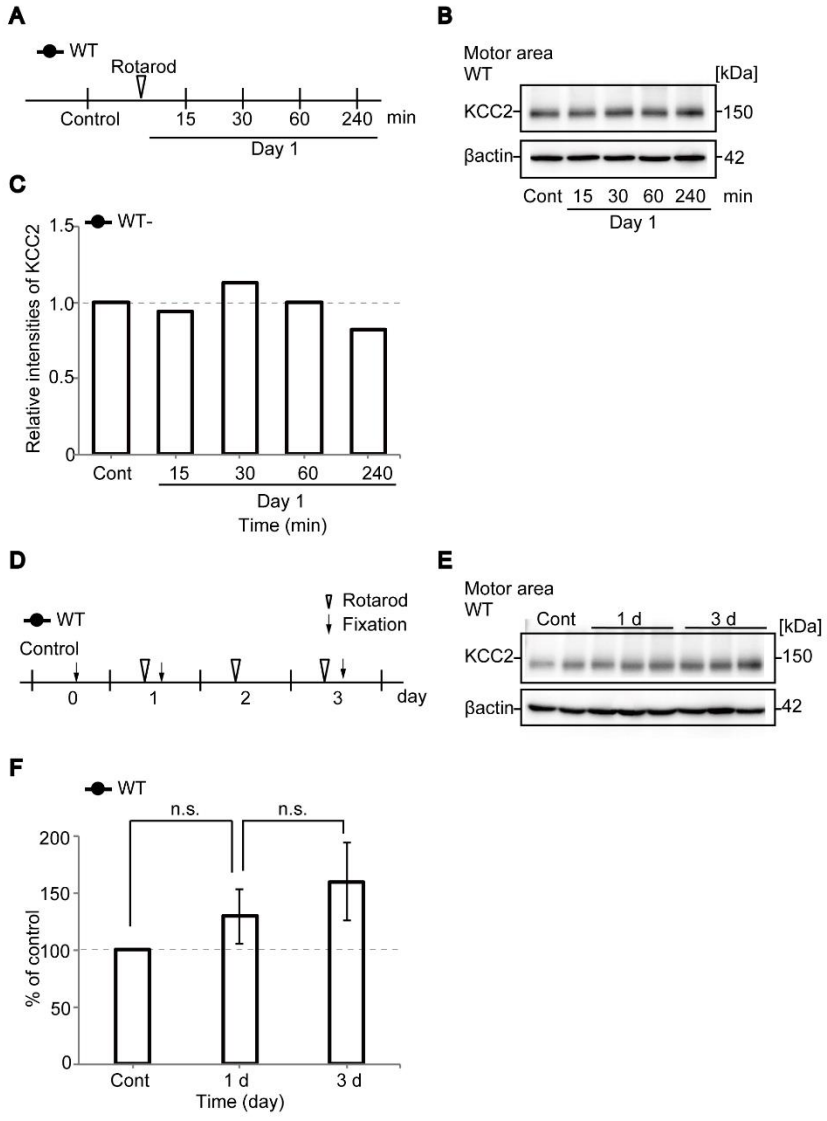
A
WT
Rotarod
Control
15
30
60
240
min
Day 1
B
Motor area
WT
[kDa]
KCC2
150
βactin
42
Cont 15 30 60 240 min
Day 1
C
WT-
Relative intensities of KCC2
1.5
1.0
0.5
0
Cont
15
30
60
240
Day 1
Time (min)
D
WT
Rotarod
Fixation
Control
0
1
2
3
day
E
Motor area
WT
Cont
1 d
3 d
[kDa]
KCC2
150
βactin
42
F
WT
n.s.
n.s.
% of control
200
150
100
50
0
Cont
1 d
3 d
Time (day)

Figure 7. KCC2 overexpression increased spine formation in pyramidal neurons *in vivo*.

Imaging was performed 2-3 weeks after making the cranial window and injecting adeno-associated virus (AAV) with eGFP. Repeated an *in vivo* imaging of their dendrites located at layer 1/2 with a two photon laser microscope has been carried out at an interval of 24 hours.

A. Timeline of imaging experiment. Changes spine structural were observed chronically before and after stopping oral administration of doxycycline. Repeated imaging performed from day -2 to 14 (refer arrowhead).

B-C. Representative images of WT mice (WT: 9 dendrites, 3 animals) (B) and KCC2 overexpressing mice (KCC2: 7 dendrites, 2 animals) (C) during day -2 to day 14. Red arrowhead shows the newly formed spines, and blue arrowhead of WT neurons eliminated spines. Scale bar is 5 μm.

D. Quantitative analysis of the temporal evolution of apical dendritic spine density. Results were expressed as mean ± standard error of mean. Red line shown the KCC2 overexpressing mice (KCC2: 7 dendrites, 2 animals), and black line is the WT mice (WT: 9 dendrites, 3 animals). Two-way ANOVA with Bonferroni post hoc test was used, and statistical differences between KCC2 and WT.

E. Quantitative analysis of spine density demonstrated significantly difference between WT and KCC2 in averaged 10 to 14 day (**$P < 0.01$, unpaired t-test).

Figure 7

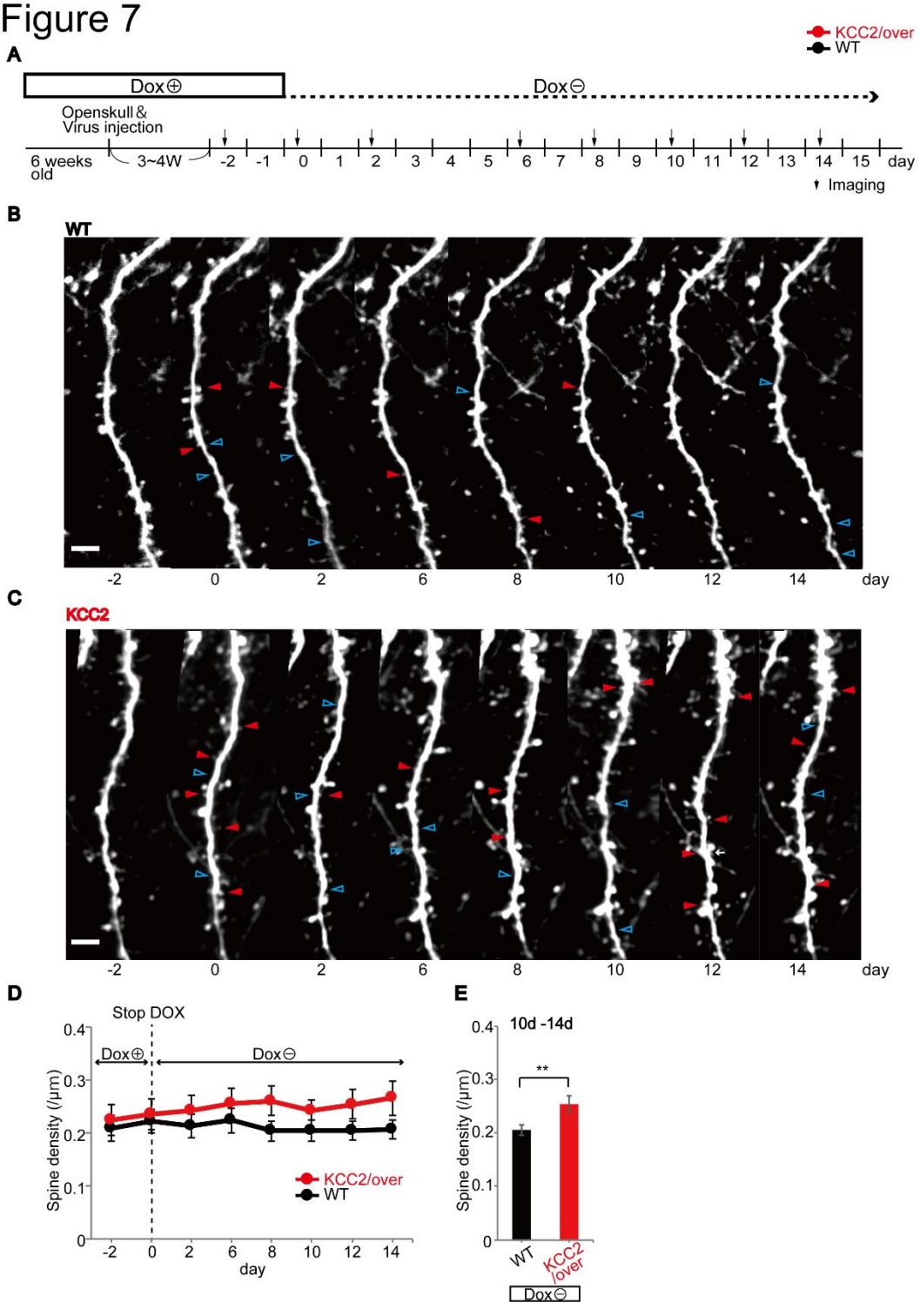
A
KCC2/over
WT
Dox⊕
Dox⊖
Openskull &
Virus injection
6 weeks
old
3~4W
-2 -1 0 1 2 3 4 5 6 7 8 9 10 11 12 13 14 15 day
Imaging
B
WT
-2 0 2 6 8 10 12 14 day
C
KCC2
-2 0 2 6 8 10 12 14 day
D
Stop DOX
Dox⊕
Dox⊖
Spine density (/μm)
0.4
0.3
0.2
0.1
0
KCC2/over
WT
-2 0 2 6 8 10 12 14
day
E
10d -14d
**
Spine density (/μm)
0.4
0.3
0.2
0.1
0
WT
KCC2
/over
Dox⊖

Figure 8. The density and turnover of spine were stable after 4 weeks removing doxycycline *in vivo*.

A. Timeline of imaging experiment. Changes spine structural were observed during 7 days after stopped doxycycline 4 weeks (refer arrowhead).

B-C. Representative images of WT mice (WT: 8 dendrites, 3 animals) (B) and KCC2 overexpressing mice (KCC2 overexpressing: 8 dendrites, 4 animals) (C). Scale bar is 5 μm.

D-F. Spine formation (D) and elimination (E) were not different between two groups, addition spine turnover (F) is also not difference.

G. Spine density in KCC2 overexpressing mice is consistently higher than that in WT mice during imaging.

H. Representative images of single dendrites in WT (left) and KCC2-overexpressing (right) mice using *in vivo* two photon imaging of dendrites and spines in apical dendrites of layer V pyramidal neurons of the motor cortex. Scale bar is 5 μm.

I. In KCC2-overexpressing mice (34 dendrites, 16 animals), there was a significant increase in spine density as compared to WT mice (18 dendrites, 11 animals ***$P < 0.001$, unpaired t-test). Graphs show individual data with means ± SEM.

Figure 8

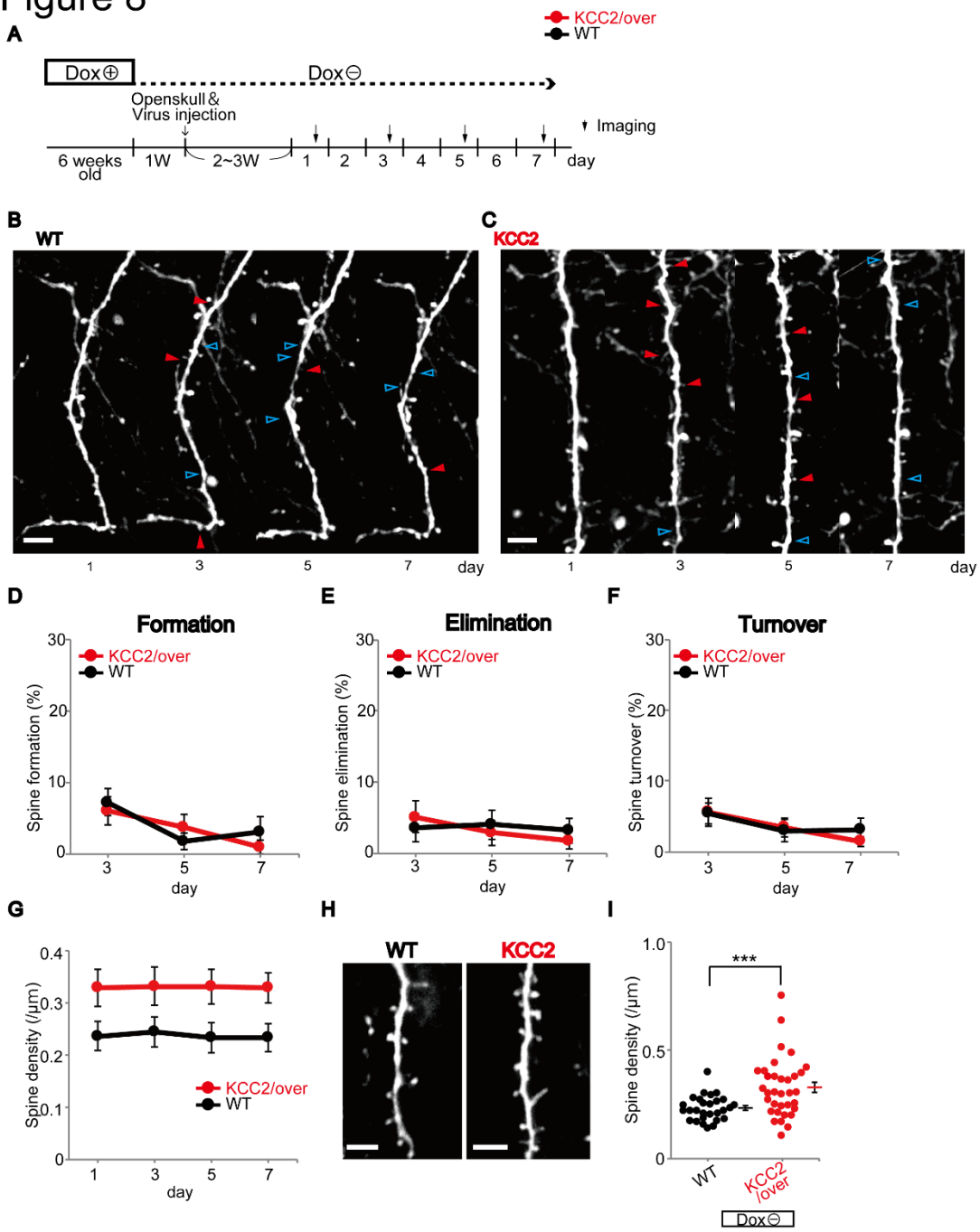
A
KCC2/over
WT
Dox⊕
Dox⊖
Openskull &
Virus injection
Imaging
6 weeks old
1W
2~3W
1
2
3
4
5
6
7
day
B
WT
C
KCC2
1
3
5
7
day
D
Formation
E
Elimination
F
Turnover
Spine formation (%)
Spine elimination (%)
Spine turnover (%)
30
20
10
0
3
5
7
day
G
Spine density (/μm)
0.4
0.3
0.2
0.1
0
H
I
***
1.0
0.5
WT
KCC2 /over
Dox⊖

Figure 9. Remodeling of spines during motor learning in KCC2 overexpressing mice and WT mice.

Using transcranial two-photon imaging method, I investigated synaptic remodeling during learning.

A. Schematic diagram of experimental protocol. Imaging and rotarod training began 3 weeks after withdrawing Dox from the diet. The same dendrites were imaged over 5 consecutive days. From days 1 to 3, rotarod training was performed in the morning prior to imaging later that day.

B-C. Representative single dendrites of pyramid neurons from WT (B) and KCC2 overexpressing (C) mice during repeated *in vivo* imaging before and during rotarod training. Red arrowheads indicate spines that newly appeared as compared to the previous day's image (newly formed spines), while blue arrowheads indicate those that disappeared (eliminated spines). Scale bars in each image in (B) and (C), 5 μm.

D. Spine density measured at each imaging day was consistently higher in KCC2 overexpressing mice as compared to that in WT mice.

E. The relative number of new spines which formed during the 1st day of rotarod learning was significantly greater in KCC2 overexpressing mice, but not in WT mice. However subsequent new spine formation rates were not different. The graph plots the percentage of spines in a dendrite which were not present at the previous day's imaging. (7 KCC2 over-expressing mice,

23 dendrites; 7 WT mice, 18 dendrites; one-way ANOVA followed by Tukey's test, 0 day vs 1 day KCC2 overexpressing mice, *$p < 0.05$).

F. The proportion of spines that disappeared (spine elimination) across the rotarod training period was not significantly different between WT and KCC2 overexpressing mice.

G. The spine turnover rate (the numerical addition of formation and elimination) was significantly increased following 1 day of rotarod training for KCC2 overexpressing mice (one-way ANOVA, Tukey's test, **$p < 0.01$), but not for WT mice - nor was it significantly different for WT or KCC2 overexpressing mice at 2 and 3 days.

Figure 9

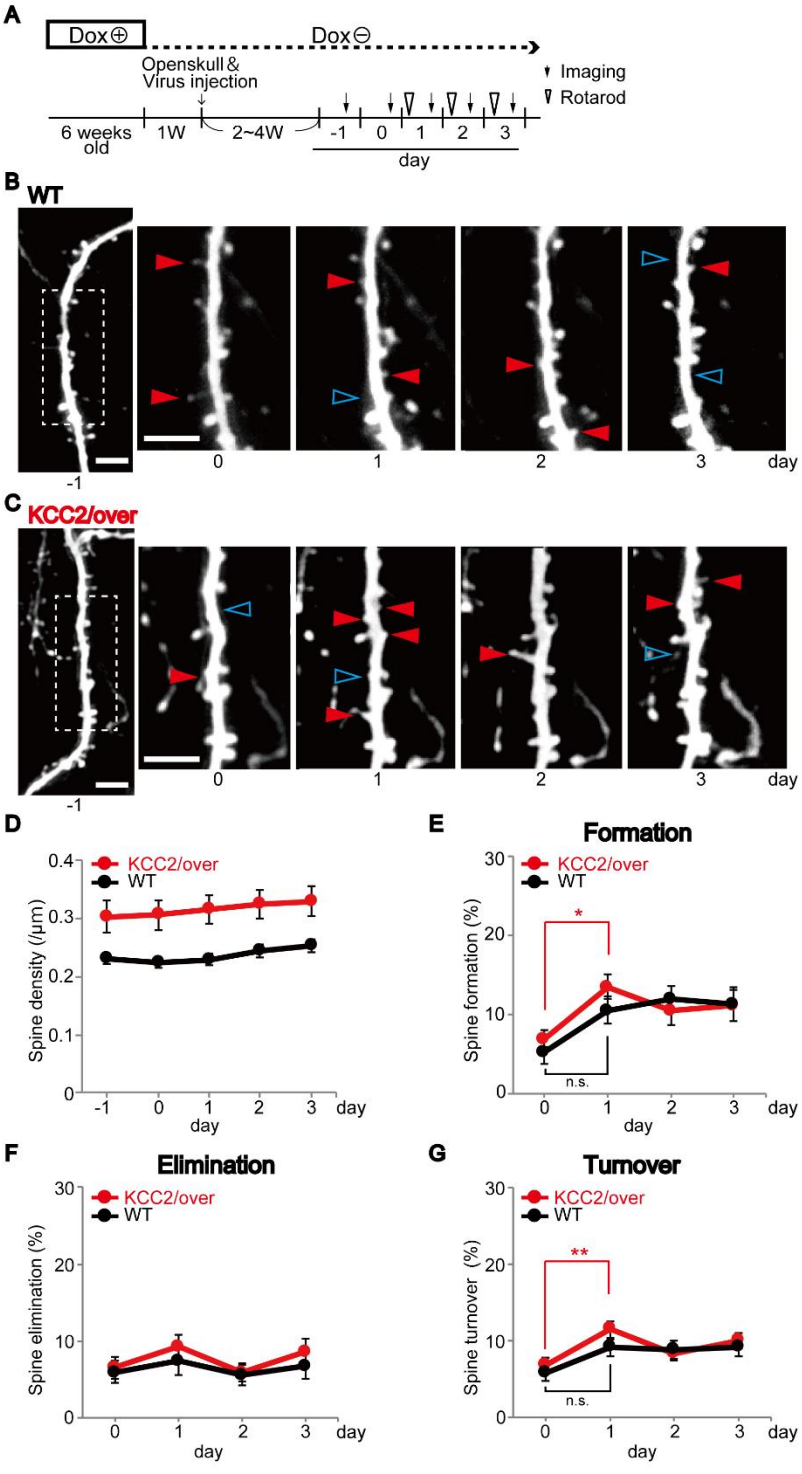
A
Dox⊕
Dox⊖
Openskull &
Virus injection
Imaging
Rotarod
6 weeks
old
1W
2~4W
-1
0
1
2
3
day
B
WT
-1
0
1
2
3
day
C
KCC2/over
-1
0
1
2
3
day
D
KCC2/over
WT
Spine density (/μm)
0.4
0.3
0.2
0.1
0
-1
0
1
2
3
day
day
E
Formation
KCC2/over
WT
Spine formation (%)
30
20
10
0
*
n.s.
0
1
2
3
day
day
F
Elimination
KCC2/over
WT
Spine elimination (%)
30
20
10
0
0
1
2
3
day
day
G
Turnover
KCC2/over
WT
Spine turnover (%)
30
20
10
0
**
n.s.
0
1
2
3
day
day

Figure 10. Stability of newly formed and existing spines.

A. Schematic of pre-existing stable spines before motor learning.

B. Survival rates of spines that existed prior to the rotarod training in both WT and KCC2 overexpressing mice, indicates a similar rate of spine elimination.

C. Schematic of the protocol used to define the stability of newly formed spines. Spines which appeared on the first day of training (closed circles, relative to 1 day pre-training) were either present (closed circle) or eliminated by the next day (open circle). Similarly new spines observed after day 2 of rotarod training (closed squares, relative to day 1) were either present (closed square) or eliminated (open square) by the next day.

D-E. The relative elimination rates of newly formed spines indicates that about 80% of the new spines survive the next day with no difference between WT and KCC2 overexpressing mice. (D), While, a more spines generated at the 1st day of training in KCC2 overexpressing mice consequently leads to a more survival of new spines in number at the 2nd day, than that of WT mice (E).

Figure 10

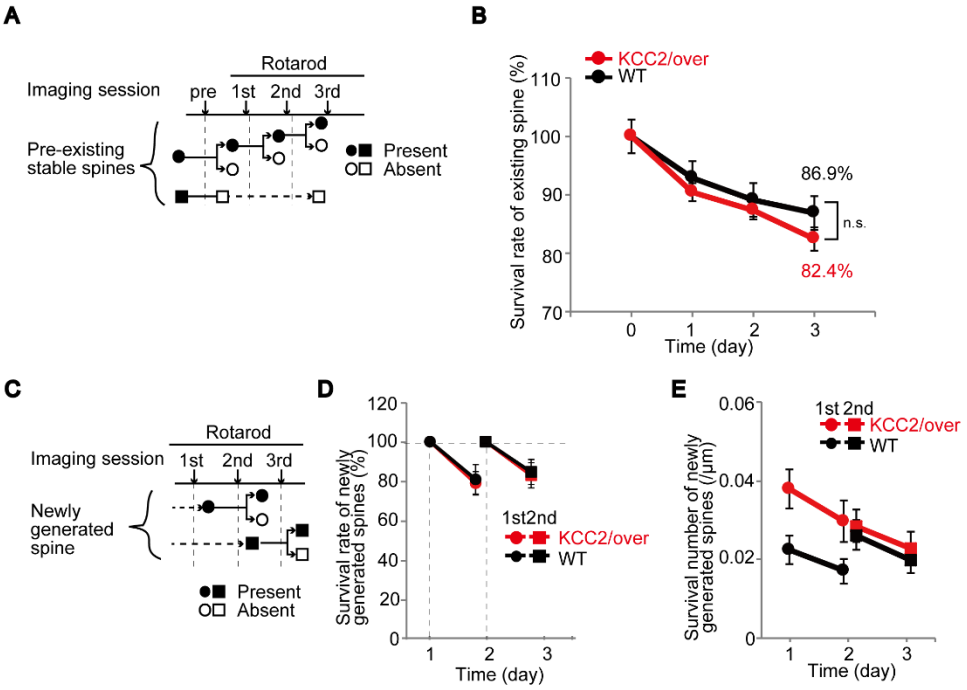
A
Rotarod
Imaging session
pre
1st
2nd
3rd
Pre-existing
stable spines
Present
Absent
B
KCC2/over
WT
Survival rate of existing spine (%)
110
100
90
80
70
86.9%
n.s.
82.4%
0
1
2
3
Time (day)
C
Rotarod
Imaging session
1st
2nd
3rd
Newly
generated
spine
Present
Absent
D
Survival rate of newly generated spines (%)
120
100
80
60
40
20
0
1st2nd
KCC2/over
WT
1
2
3
Time (day)
E
Survival number of newly generated spines (/μm)
0.06
0.04
0.02
0
1st 2nd
KCC2/over
WT
1
2
3
Time (day)

Figure 11. Increasing new spine formation in motor learning enhanced the preparation to improvement of behavior.

A. The ratio of newly formed spines at 1st day in WT mice to the total spines shown a high correlation with the rate of improvement of motor skill in 1st day ($p = 0.01$, $r = 0.87$, $n = 7$ mice).

B. WT mice which has less number of new spine formation, showed no association ($p = 0.5$, $r = 0.3$, $n = 7$ mice).

C. The ratio of newly formed spines of KCC2 overexpressing mice to the total spines at 1st day of training co-relates with an improvement of motor performance at the 2nd day ($p = 0.07$, $r = 0.7$, $n = 7$ mice).

Figure 11

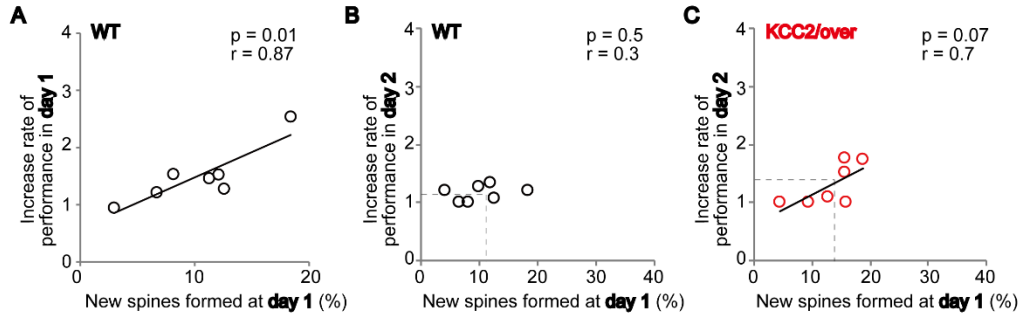
A
WT
p = 0.01
r = 0.87
Increase rate of performance in day 1
New spines formed at day 1 (%)
B
WT
p = 0.5
r = 0.3
Increase rate of performance in day 2
New spines formed at day 1 (%)
C
KCC2/over
p = 0.07
r = 0.7
Increase rate of performance in day 2
New spines formed at day 1 (%)

Figure 12. KCC2 enhances activity dependent synaptic plasticity and learning.

A. In results, using a conditional transgenic mouse strategy, I examined whether overexpression of KCC2 enhances dendritic spines in the adult nervous system, and characterized the effects on spine dynamics in the motor cortex *in vivo* during rotarod training. I have shown that: 1) increasing KCC2 in the brain after the major developmental period of synaptogenesis can increase dendritic spine density (upper red), 2) that increasing KCC2 enhances the capacity of motor learning to form new dendritic spines, and 3) increasing KCC2 increases the extent and rate of performance increase during training (upper and under red). Hence my data strongly supports the growing appreciation of the role of KCC2 in dendritic spine development, maturation and/or maintenance, and extends this to a putative role in enhancing synaptic plasticity and performance during learning *in vivo*.

Figure 12

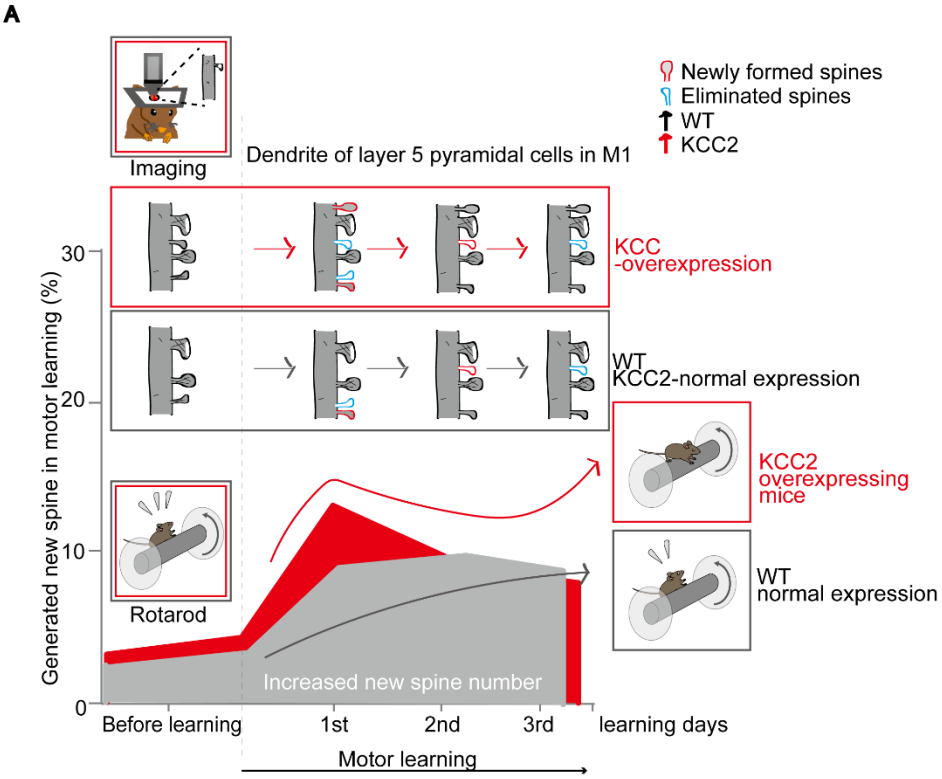
A
Newly formed spines
Eliminated spines
WT
KCC2
Imaging
Dendrite of layer 5 pyramidal cells in M1
KCC
-overexpression
WT
KCC2-normal expression
KCC2
overexpressing
mice
WT
normal expression
Rotarod
Generated new spine in motor learning (%)
30
20
10
0
Increased new spine number
Before learning
1st
2nd
3rd
learning days
Motor learning